EUROPEAN ORGANIZATION FOR NUCLEAR RESEARCH

CERN–PPE/92–125
SL MD Note 25
31 July 1992

The Energy Calibration of LEP in 1991

The working group on LEP energy

L. Arnaudon[1], R. Assmann[2], J. Billan[1], W. Birr[1], A. Blondel[3], G. Bobbink[1,4], F. Bordry[1], H. Burkhardt[1], M. Crozon[5], B. Dehning[2], A. Faugier[1], J. Gascon[6], R. Giachino[1], A. Grant[1], J.P. Gourber[1], J.L. Harton[7], V. Hatton[1], C.M. Hawkes[1], K.N. Henrichsen[1], A. Hofmann[1], R. Jacobsen[1], L. Knudsen[1], J.P. Koutchouk[1], G. Musolino[1], S. Myers[1], R. Olsen[1], J. Panman[1], E. Peschardt[1], M. Placidi[1], D. Plane[1], G. Quast[8], A. Read[1], L. Rolandi[1], R. Schmidt[1] and H. Wachsmuth[1]

Abstract

This report summarizes the measurements providing the absolute energy calibration of the LEP beam during the energy scan of 1991. The results of the magnetic measurements are given including the corrections needed for temperature differences. A summary of the polarization measurements is given, together with the measurements of the circumference of the ring, and the energy measurements with protons. A description of these measurements and of the corrections to be made to them is given, addressing the problem of uncertainties in these results. The availability of the energy measurements with resonant-depolarization improves the precision of the result significantly. The result is a calibration of the energy of the beam, with a precision of $2\sigma(E_{beam}) = 5.3$ MeV at $2E_{beam} = 93$ GeV. For the data taken in 1991, it is concluded that the systematic uncertainty in the Z-mass due to the energy calibration is about 6.3 MeV, and in the Z-width is about 4.9 MeV.

Submitted to the
XXVIth International Conference on High Energy Physics,
Dallas, Texas, USA

1) CERN, 1211 Geneva 23, Switzerland
2) Max Planck Institut für Physik und Astrophysik, Werner-Heisenberg-Institut für Physik, 8000 Munich, Germany.
3) Laboratoire de Physique Nucléaire des Hautes Energies, Ecole Polytechnique, IN^2P^3-CNRS, 91128 Palaiseau Cedex, France.
4) NIKHEF, Postbus 41882, 1009 DB Amsterdam, The Netherlands.
5) Laboratoire de Physique Corpusculaire, Collège de France, IN^2P^3-CNRS, 75231 Paris Cedex, France.
6) Laboratoire de Physique Nucléaire, Université de Montréal, Montréal, Quebec, H3C 3J7, Canada.
7) Department of Physics, University of Wisconsin, Madison, WI 53706, USA.
8) Universität Hamburg/DESY, II Inst. für Experimentalphysik, 2000 Hamburg 52, Germany.

Contents

1 Introduction

During the 1991 running period of LEP an energy scan was performed in order to improve the measurement of the mass of the Z and its width. This required a larger number of Z decays and a better absolute calibration of the energy of the LEP beams [1]. This report concentrates on the improvements in the measurement of the absolute energy of the beams. Some new tools became available, new methods were developed and several new effects were found.

After the successful observation of polarization of the electron beam in 1990 [2] several measurements of the beam energy were performed using the resonant-depolarization method [3]. These measurements are much more precise than any of the measurements available in 1990, and form the corner-stone of the energy calibration for the run in 1991. These experiments determine the average azimuthal energy, which is related to the spin precession per revolution ("the average energy of the particles in the arcs").

The energy scan was organized in a slightly different way compared to the 1990 scan. The energy points were chosen to optimize the probability for polarization of the beams at as many energy scan points as possible. Practical constraints were the 440 MeV periodicity of the optimum polarization energies (with a tolerance of ± 50 MeV) and the 125 MeV minimum step in the energy ramp (both in terms of beam energy). Thus the nominal beam energies were chosen as shown below:

label	nominal energy [GeV]	expected polarization
-3	44.250	$-$
-2	44.750	$-$
-1	45.125	$-$
PEAK	45.625	$+$
$+1$	46.000	$+$
$+2$	46.500	$+$
$+3$	46.875	$+$

For the optics of LEP in 1991, energies where polarization is expected are marked with "+", while at energies marked "−" no polarization is expected for these optics.

In 1991, the resonant-depolarization method was developed and experiments were carried out at one energy (the "+2" setting). The energy scan started at 5 August, with fill number 727 and ended at 11 November with fill number 866. One energy scan cycle consisted of cross-section measurements at each of the off-peak points interspersed with peak points. Five such scans were performed, with a total integrated luminosity of around 1 pb^{-1} at the off peak points and 4.5 pb^{-1} on the peak.

A better understanding of the variations observed in the flux-loop measurements was obtained. In particular the effects of temperature variations on the flux-loop measurements were clearly demonstrated [4]. Laboratory measurements were needed to assign these variations to actual changes of the magnetic fields in the magnets for a given excitation current. These observations led to a temperature-dependent correction to the flux-loop measurements, which produced a much more regular behaviour of the magnetic field as a function of the calendar time. However, a sudden change in the time variation of the flux-loop measurements was observed after mid-August 91, and is little understood.

The polarization data are used as the main ingredient with many supporting measurements, such as the "field display" system, to transport the measurements in time, temperature measurements and the measurements of the temperature-dependent effects, the magnetic measurements to monitor the stability and ageing of the magnets and the combination of proton measurements with the magnetic measurements and the polarization measurements to understand non-linearities.

Two other effects leading to a variation of the energy of the beams have been identified. The first is a the local modification to the collision energies in individual interaction points (IP), driven by the alignment errors of the LEP radiofrequency (RF) system; the second related to the tidal forces which has been shown to have an effect which could modify the energy of the beams to a non-negligible degree [5].

In this report a consistent approach to arrive at an absolute calibration of the beam-energy is developed.

The calibration of the absolute energy scale was obtained as follows:

- For each fill the field in the reference dipole was measured with the field display system, yielding a reference energy, E_{FD}.
- The energy measured by the resonant-depolarization method determined the absolute energy scale at the 46.5 GeV beam energy setting relative to the field display value.
- A local scale correction was applied to derive the energy difference of the other scan points compared to the 46.5 GeV setting. This correction was derived from the flux-loop measurements.
- A temperature dependent correction is applied on a fill-by-fill basis. The effective temperature of the dipoles was estimated using the average temperature of a set of eight magnet blocks in the ring. The

temperature coefficient was obtained by flux-loop measurements and from dedicated experiments in the laboratory.
- An interaction-point dependent correction was determined taking into account the alignment errors of the RF-cavities and the voltage distribution in these cavities. This correction varied in time.

The final result of this procedure is a table with the best estimate of the centre-of-mass energy for each fill and for each interaction region.

The uncertainties in the determination of the absolute energy were divided into different categories:
- The uncertainty in the absolute energy scale.
- The uncertainty in the local energy scale.
- Uncorrelated energy-point-to-energy-point errors.
- Fill-to-fill non-reproducibility errors.

We first discuss the results of the measurements needed to calibrate the LEP beam energy (Section 2). This includes the field display system, and magnetic, polarization and radio frequency measurements. In Section 3, IP-dependent effects induced by the RF-system are summarized. Section 4 describes corrections such as the earth field, tidal variations and the effect of corrector dipoles. Comparisons between various energy-calibration methods are made in Section 5. Section 6 gives the final calibration results, with conclusions in Section 7. Some important reference material is contained in the appendices.

2 Measurements

2.1 Field display system

The magnetic field of the bending magnets in LEP is monitored hourly with a measurement of the field in a reference dipole magnet, which is connected in series with the ring magnets. This reference magnet is kept in a well controlled environment with temperature stabilization. Unlike the main ring magnets, the reference magnet does not contain mortar. It is constructed from the same dipole laminations, held in a special frame, thus ensuring that the magnet does not age in the way that the ring magnets age.

The energy estimated from this reading is labeled E_{FD} and is used as a reference, with which to compare all other measurements. It acts as a precise current meter, with the added benefit of a sensitivity to hysteresis effects which are experienced by the LEP magnets.

The magnetic field strength in this magnet is measured regularly by means of a flip coil [6] mounted in the magnet gap along the theoretical position of the central orbit. The reproducibility of this measurement is about 2.5×10^{-5} (RMS) over a short dynamic range and over the time relevant for the energy scan data. The resolution over short time intervals (e.g. during a coast) is better than 10^{-5}. A measurement is performed automatically at regular intervals during the physics coasts and can be requested at any time through the LEP control system.

The stability of the electronic integrators used in this system was regularly checked, and the field display value was found to be consistent over long periods of time with the direct measurement of the current supplied to the dipoles, within 5×10^{-5}.

2.2 Magnetic measurements

A considerable effort has been spent on magnetic measurements of the LEP dipoles, both before installation in the ring and interspersed with the three years operation of the machine. In addition, auxiliary laboratory measurements have been performed to monitor the long term behaviour on a set of spare magnets and to check temperature dependent effects.

The cores of the dipole magnets are made of steel laminations, spaced at regular intervals. The space between the laminations is filled with cement mortar. The change of water content of the mortar filling has an effect on the magnetic properties of the cores. This causes a slow ageing of the dipole cores, visible in the measurements of the bending strength. The effect is understood to be a result of stresses induced on the iron laminations [7]. Temperature differences can also induce stresses in the cores, and hence are expected to have some influence on the magnetic properties of the dipoles.

2.2.1 Measurements prior to installation

Each of the 3280 dipole cores has been equipped with a "flux-loop" made of thin copper wires embedded in grooves machined in the lower poles. The magnetic properties of all dipoles have been determined prior to installation by means of rotating coils in the center of the gap, at the theoretical position of the central orbit of the beams. At the same time, these measurements were compared with the induced voltage in the embedded flux-loops when the current in the dipoles was changed. This procedure provides an effective calibration of the area of the flux-loops in each core. The dipole cores were calibrated without the beam vacuum tube inserted.

The calibration of the flux-loops were performed on a magnetic cycle between +2900 A and −2900 A (equivalent to +60 and −60 GeV) with a precision of 10^{-4} of full scale, i.e. a 6 MeV precision.

2.2.2 Measurements of the "Nickel-effect"

The vacuum pipes fitted in the space between the poles of the dipoles contain a $\approx 7\mu$m thick layer of nickel used for the bonding of the aluminium pipes with a lead radiation shield.

Table 1: Measurements of the effects on the magnetic field measurement with the flux-loop of the nickel on vacuum pipes. The first column gives the interval in terms of effective current in the magnet, the second column the difference between the measurements of a bare core and a core with vacuum pipe and shims as measured with the flux-loop in Gauss, the third column gives the correction to be applied to the measurement in the tunnel in terms of beam energy in MeV.

Interval	measured change	$\Delta_{FD} - \Delta_{FL}$[MeV]
Remanent field	−0.20 G	-19
$I = 0 \rightarrow I = 300$A	+0.09 G	+9
$I = 300$ A $\rightarrow$ 20 GeV setting	+0.04 G	+4
$I = 300$ A $\rightarrow$ 45 GeV setting	+0.09 G	+9
$0 \rightarrow 20$ GeV (incl. remanent field)		-6 ± 5
$0 \rightarrow 45$ GeV (incl. remanent field)		-1 ± 6
20 GeV $\rightarrow$ 45 GeV		$+5 \pm 5$

The nickel has a substantial influence on the effective strength of the dipole as felt by the particle beams. In order to compensate for this effect shims were fitted in the poles. The effect of this is visible as a change of the remanent field, of the effective gap thickness (the nominal gap size is 100 mm), and a redistribution of flux-lines.

Measurements were performed to evaluate the difference between the empty dipoles and those including the vacuum pipe and the shims. The aim of these studies was to find a correction to the response of the flux-loop, since the only magnetic measurements available in the tunnel are obtained with this device. The procedure was to measure the field at the theoretical central orbit with a rotating coil and compare this with the embedded flux-loop. The effect of the nickel and the shims is to change both measurements; the correction to be applied to the data from the flux-loop measurements in the tunnel is then the double ratio of the two measurements with and without vacuum chamber. The data are summarized in Table 1.

Only one vacuum chamber could be used for the measurements. The thickness of the nickel layer of one-eighth of all chambers was measured, and the average thickness was found to coincide with the thickness of the layer of the measured chamber.

2.2.3 Ageing of the flux-loop

The calibration of the flux-loops have changed since the time of their first calibration prior to installation in the ring, due to the shrinkage of the dipole cores with dehydration. The ageing is monitored regularly using a set of spare dipoles as a reference.

In fact, there are two partially canceling changes to the flux-loop calibration due to the shrinkage of the cores. One component is the change of the surface area over 4.5 years, which is measured to be

$$\frac{\Delta E_{FL}}{E} = -\frac{\Delta S}{S} \simeq -4 \times 10^{-4} \tag{1}$$

where the 4.5 years are the average time between the calibration of the loops and the 1991 energy scan.

The other component is the change in core length induced by the shrinkage. Owing to the details of the installation of the magnets on their supports in the tunnel, only on-half of the core-shrinkage translates into a magnetic length change. The gap between the two dipoles of a pair mounted on a common support takes up one-half of the shrinkage. This gap has a field strength almost equal to the field inside the cores. The resulting size of the variation is

$$\frac{\Delta E_L}{E} = 0.5\frac{\Delta L_{core}}{L_{core}} \qquad \text{while} \qquad \frac{\Delta L_{core}}{L_{core}} \simeq 0.5\frac{\Delta S}{S} \tag{2}$$

Thus this correction has the opposite sign and one-quarter of the magnitude of the surface shrinkage term.

The net effect is a decrease of the flux-loop response of

$$\Delta C_{FL}/C_{FL} = (-3 \pm 1) \times 10^{-4}, \tag{3}$$

for which the flux-loop results have to be corrected.

2.2.4 Non-linearities of the magnets

The present calibration of the Field Display is based on the systematic magnetic measurements of all dipole cores including estimated ageing effects. The original relation between E_{FD} and the magnetic field in the dipoles ("transfer function") was linear. However, both the remanent field of the dipole magnet and the permeability of its laminations at a given temperature have changed with time. So the variations of the dipole excitation curve are not linear. At present a non-linearity of about -2×10^{-3} is observed with respect to the reference magnet in the region of 45 GeV, i.e. a requested change of 1 GeV gives an energy change of only 0.998 GeV. The transfer function could be linearized and updated, but since it is preferable to use the original data in the control system the transfer function is not changed and a correction is applied of the form:

$$\Delta E_{CM} = \alpha \ (2E_{FD} - 93.0 \text{ GeV }) \tag{4}$$

where α is a time dependent local energy scale parameter. The best estimate of α for the different running periods is:

$$\alpha = (-2.0 \pm 1.5) \times 10^{-3}. \tag{5}$$

The uncertainty in the local energy scale can be estimated comparing proton data at 20 GeV and polarization data at 45 GeV with the flux-loop measurement for this energy difference (see section 5).

2.2.5 Flux-loop measurements in the ring

Regular flux-loop measurements of the field in the LEP dipoles have been performed since October 1989. The flux-loops of the individual magnets are connected in series, throughout each of the octants of LEP. The measurements are performed by applying a symmetric current cycle between +2900 A and −2900 A, corresponding to ±60 GeV, and integrating the induced voltage in the flux-loops with eight digital integrators [7], [8], [9].

The measurements are shown in Fig. 1. The data at the 45 GeV setting show a slowly decreasing strength caused by the ageing process. However, this effect is somewhat obscured by large point-to-point fluctuations; at the 20 GeV setting no ageing is observable. The results of all flux-loop measurements are given in Appendix A. To investigate these fluctuations, temperature sensors were installed on some of the dipoles in LEP.

2.2.6 Temperature dependence of the flux-loop measurements

A detailed account of the study of temperature dependent effects on the measurements with the flux-loop is given in [4]. A continuous monitoring of the temperature of a sample of four magnets was installed in June 1991. Temperature variations from 17 ^{o}C up to 23 ^{o}C were observed, the high temperatures corresponding to occasions when the magnets had been powered in the period preceding the measurements, while the lowest values were observed during interruptions in the running of the machine. In addition, differences of up to two degrees were observed in the absolute value of the temperature of different magnets.

A correlation between the flux-loop measurements and the measured temperature was clearly demonstrated with a controlled experiment, in which many successive flux-loop measurements were performed, during a cooling-down period after steady operation of the machine (see Fig. 2).

A temperature correction to the flux-loop measurements was obtained with a value

$$(1.01 \pm 0.25) \times 10^{-4} \text{ per } {}^o\text{C} \text{ at 45 GeV}, \tag{6}$$

and

$$(0.59 \pm 0.15) \times 10^{-4} \text{ per } {}^o\text{C} \text{ at 20 GeV}. \tag{7}$$

Fig. 1 shows the flux-loop data as a function of time corrected for the different temperatures at which they were taken.

For LEP operation before June 1991, the magnet temperature had not been monitored. Therefore a model was developed which was able to predict the effective temperature of a given magnet or a set of magnets given the history of the current applied to the dipoles.

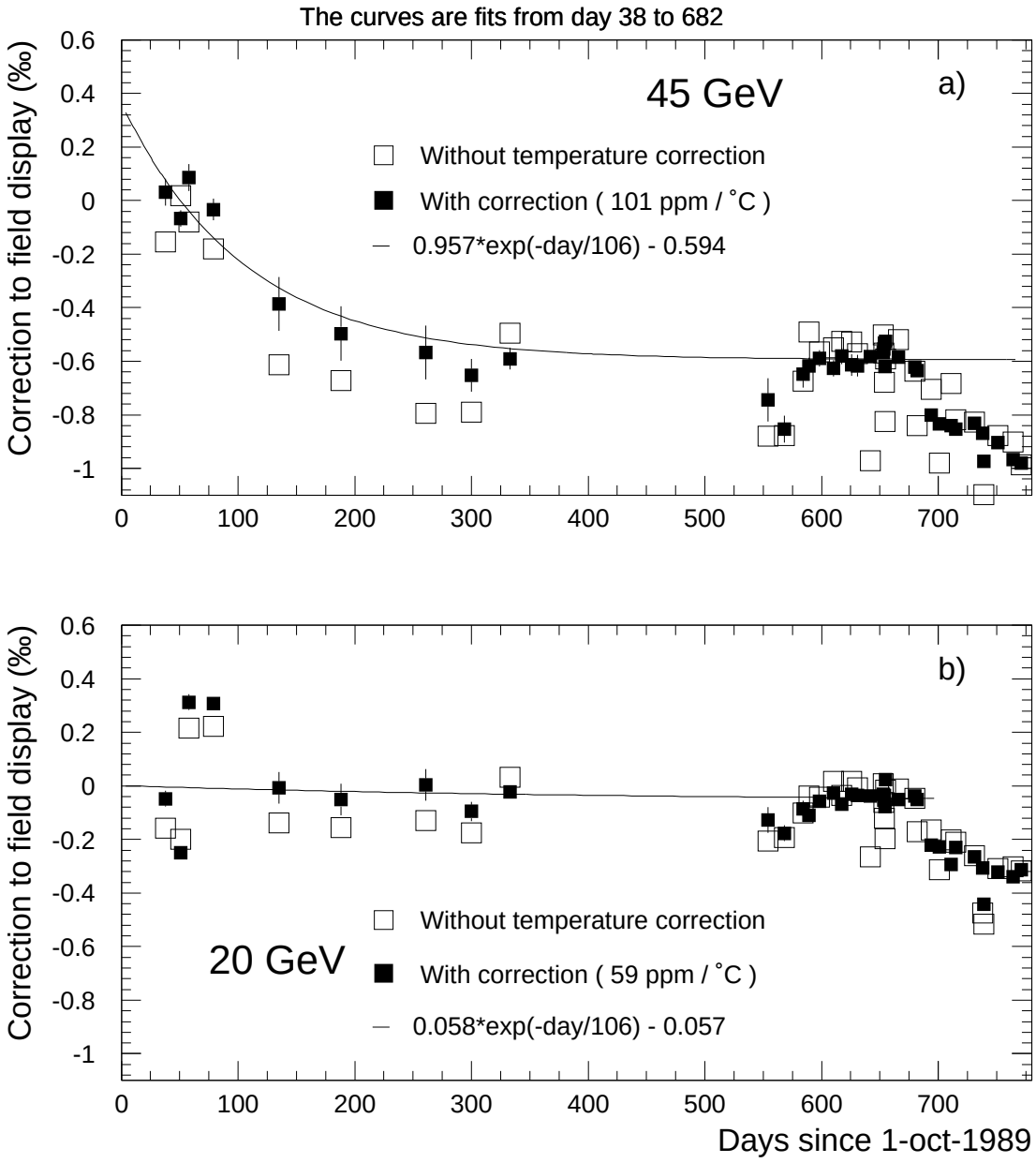

Figure 1: (a) Correction of the field display at 45 GeV, determined from flux-loop measurements, as a function of time after October 1^{st}, 1989. Open squares: data before the temperature correction; closed squares: data after being corrected for the temperature dependence. All points are projected to a temperature close to that of normal running condition (22.25 °C). The error bars take into account the uncertainty on the temperature correction only. The line is an exponential decay adjusted to the corrected data, representing the ageing of the magnets, fitted to the data before 14 August, 1991 (day 682). (b) Same as (a), for the correction of the field display at 20 GeV.

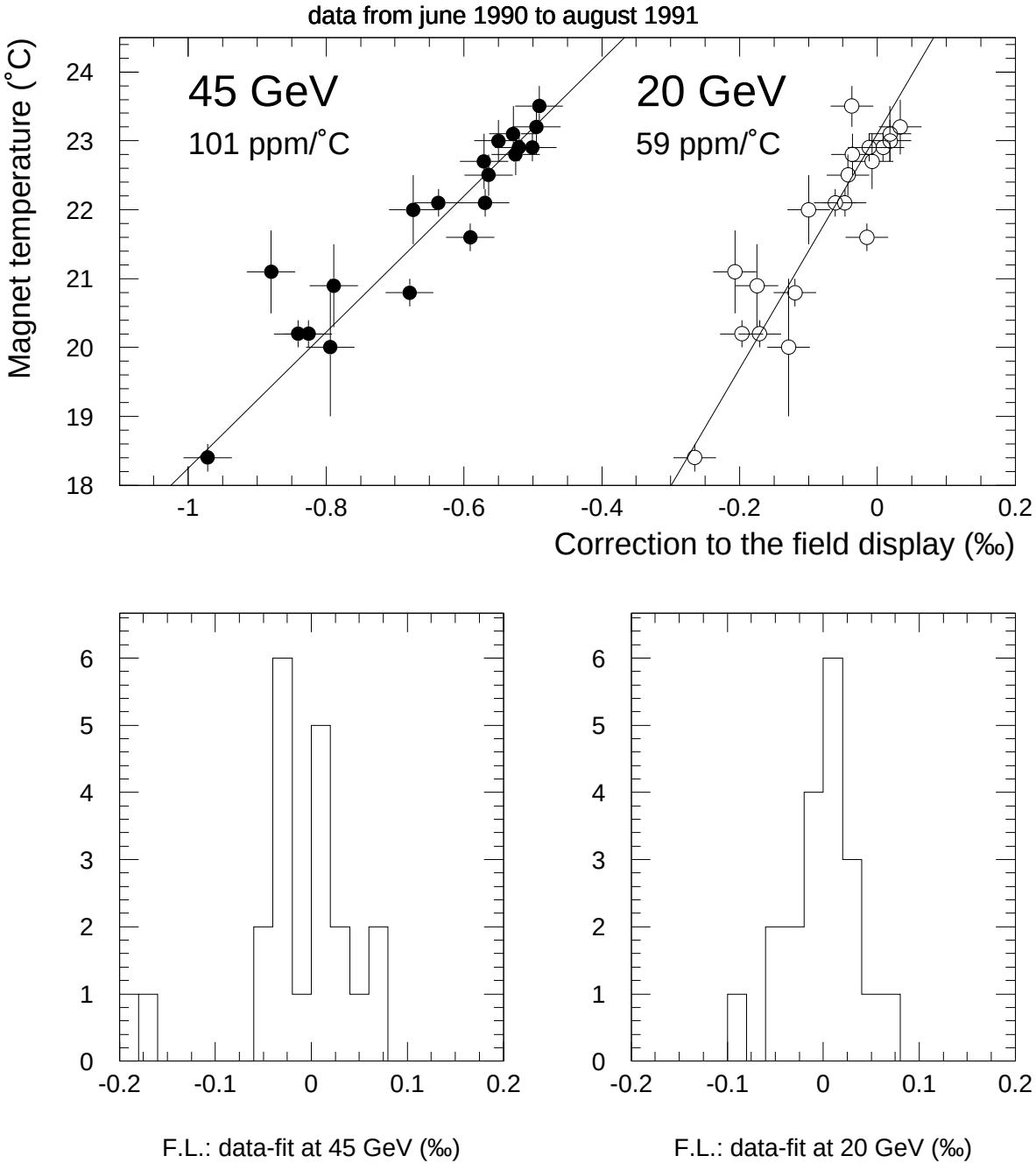

Figure 2: (top) Magnet temperature as a function of the measured correction ($\times 10^{-3}$) to the field display at 20 GeV (open circles) and 45 GeV (closed circles). (left) Fit residuals for the 45 GeV data. (right) Fit residuals for the 20 GeV data.

Table 2: Measurements of the effects of temperature differences on the LEP dipole cores. TB is the temperature coefficient of the magnetic field in the centre of the dipole, TSfl the temperature coefficient of the flux-loop surface (measured in a cycle between 20 and 60 GeV equivalent current), TL is the longitudinal expansion coefficient and TG is the transverse expansion coefficient of the dipole gap. TE, the estimated beam energy temperature coefficient is the sum of TB and 0.63 × TL. One-half of the elongation has to be added for the field change at the end of a pair, but only one-third of the other half has to be added for the smaller field change in the 50 mm gap between two cores of a pair.

Core number	TB (45 GeV) 10^{-4}	TSfl (20-66 GeV) 10^{-4}	TL 10^{-4}	TG 10^{-4}	TE (45 GeV) 10^{-4}
1684	1.09	0.40	0.13	0.20	1.17
2006	1.03	0.31	0.12	0.10	1.11
126	1.18	0.37	0.11	0.12	1.25
113	1.51	0.30	0.13	0.07	1.59
2111	0.98	0.22	0.14	0.08	1.07
1614	1.22	0.40	0.12	0.15	1.30
110	1.22	0.35	0.13	0.13	1.30
1246	1.46	0.21	0.13	0.11	1.54
108	1.34	0.30	0.15	0.13	1.43
2110	1.62	0.35	0.13	0.09	1.70
2129	0.78	0.13	0.12	0.09	0.86
2144	0.95	0.26	0.10	0.09	1.01
average	1.20	0.30	0.13	0.11	1.28
r.m.s.	0.25	0.08	0.01	0.03	0.25

The temperature coefficients thus obtained do not depend critically on the choice of magnet used to extract the temperature dependence. It is, however, better to choose the average of a set of magnets as a reference. One can then expect to have a more representative sampling of the effective temperature of all dipoles in the ring. The measurement of the temperature of such a set of eight magnets has been available since July 1991. This set of magnets has been adopted as the reference, and will be called T_8. The uncertainty in the fitted temperature coefficients was estimated to be $\simeq 25\%$ by choosing different sets of temperature-reference magnets and different periods over which the flux-loop data were taken.

Whether this correlation between the temperature of the magnets and the measurements of the flux-loop is due to a change of the excitation of the magnet or due to an instrumental effect in the flux-loop measurement can not be decided on the basis of these data. It is expected that the flux-loop response changes as function of the temperature of the magnet block due to expansion effects. On the basis of material properties, this effect is expected to be too small to explain the size of the correlation observed.

2.2.7 Laboratory measurements of the temperature dependence

In order to check whether the temperature dependence of the flux-loop measurements in the LEP tunnel are due to changes in the magnetic field or to instrumental effects, a laboratory test has been set up.

The magnetic characteristics of twelve dipole cores were measured over a temperature interval from 18 °C to 30 °C and a current in the excitation loop corresponding to an interval from 20 to 100 GeV beam energy. Measurements of the magnetic field in the centre were performed with a rotating coil, and compared with the measurement with the embedded flux-loop. Also the geometrical changes of the cores in the transverse and longitudinal direction were measured. The results are given in Table 2.

The measurements show a clear temperature dependence of the magnetic field, with a magnitude comparable to the temperature coefficients observed in the LEP tunnel, and confirm the observations done with the flux-loop. The temperature dependence of the beam energy is the sum of the effect on the central field (TB) and 63% of the elongation effect (TL); the elongation changes the size of the gap between two magnets of a pair and hence the field in this region is changed by only a small amount. The result is:

$$(\Delta E/\Delta T)_{LAB} = 1.28 \times 10^{-4} \text{ per } {}^{o}\text{C}. \tag{8}$$

In order to compare this result with the measurement with the flux-loop (eq. 6), the latter has to be corrected for the change of the flux-loop surface and 63% of the longitudinal expansion of the magnet,

$-(TSfl - 0.63TL) = 0.22 \times 10^{-4}$ per ^{o}C, and therefore, using eq. 6:

$$(\Delta E/\Delta T)_{RING} = 0.79 \times 10^{-4} \text{ per } ^{o}\text{C}. \quad (9)$$

The difference of the two estimates can be due to the different temperature gradients in the LEP-tunnel compared to the laboratory set-up, the representativity of the twelve dipole cores in the laboratory for the magnets in the ring (the r.m.s. spread of the data is large for the set of magnets), and the systematic uncertainty in the determination of the temperature coefficient of the flux-loop measurements in the ring. Section 2.2.9 describes how the two methods are combined.

2.2.8 Interpretation of a change of the flux-loop results

After temperature correction the flux-loop data taken between February 1990 and mid-August 1991 follow a smooth curve with r.m.s. fluctuations smaller than 5×10^{-5}.

The 1991 energy scan started 5 August, when the temperature-corrected flux-loop response appeared to be stable. At that time, an improvement was made to the magnet cooling system in order to keep the magnet temperatures more constant. Unfortunately the flux-loop measurements since that time show a change (see Fig. 3) to lower values. We consider two interpretations of this behaviour:

Hypothesis I If the cooling change resulted in a sudden change of the average magnet temperature relative to the measured temperature, then a break in the temperature-corrected flux-loop measurements might be expected. This situation is represented by using a constant magnet calibration for the period after 14 August.

Hypothesis II Alternatively the cooling change might have caused an accelerated ageing of the dipole cores; then a different ageing slope might be expected, possibly in addition to a step in the behaviour.

An additional complication arises when one takes into account that many measurements in 1991 could only be performed on seven out of eight sectors of the ring; the sector 3 data were often invalid because of an electrical short in one of the loops. Although a correction was applied to account for the missing measurement, it cannot be excluded that part of the step is due to the inclusion of extrapolated values for sector 3 instead of the actual measurements of that sector into the data. Indeed, the data for the seven sectors for which the measurements were always available show a more smooth behaviour, and do not show a step. This fact makes the hypothesis of a step-wise change of magnetic strength improbable. Nevertheless, we use the two hypotheses to estimate the size of possible systematic uncertainties.

The two aforementioned hypotheses are illustrated by the straight lines drawn on the plots of Fig. 3. The total reduction in centre-of-mass energy since the scan started was a step on 14 August of about -3.0×10^{-4} for the first hypothesis and a slope with a step of about -2.0×10^{-4} at the break (August 14) and a value of about 3.9×10^{-4} lower than the value before the break at the end of the scan (11 November) for the second hypothesis.

date	hypothesis I	hypothesis II
before 14 August	-0.586×10^{-3}	-0.586×10^{-3}
14 August	-0.886×10^{-3}	-0.776×10^{-3}
16 September	-0.886×10^{-3}	-0.849×10^{-3}
11 November	-0.886×10^{-3}	-0.973×10^{-3}

The dates in the table are chosen to coincide with the change in flux loop measurements (14 August), the first polarization run (16 September) and the end of the running period (11 November).

Our data, including the polarization results, do not permit to choose between one or the other hypothesis. A systematic error can arise from the fact that the integrated luminosity was not evenly distributed over the period for all the energy points in the scan.

The data taken before 14 August contain one fill at energy point "-1". This fill represents 10% of the total data taken at this energy, which could change the mean energy of this particular nominal energy point by up to 3 MeV. A little shift in energy for the data taken at the peak does not influence the mass measurement. The influence of these changes has been calculated feeding both hypotheses into the fit to the Z line shape. It is concluded that an uncertainty of $\Delta E_{CM} = \pm 2$ MeV covers the different interpretations of the variation of the flux-loop measurements. The choice of one or the other hypothesis induces a change in the width of $\simeq 1$ MeV.

2.2.9 Treatment of temperature effects

We have chosen to apply the temperature correction to the beam energy with a magnitude of

$$\Delta E/E = (1.0 \pm 0.25) \times 10^{-4} \text{ per } ^{o}\text{C at 45 GeV}, \quad (10)$$

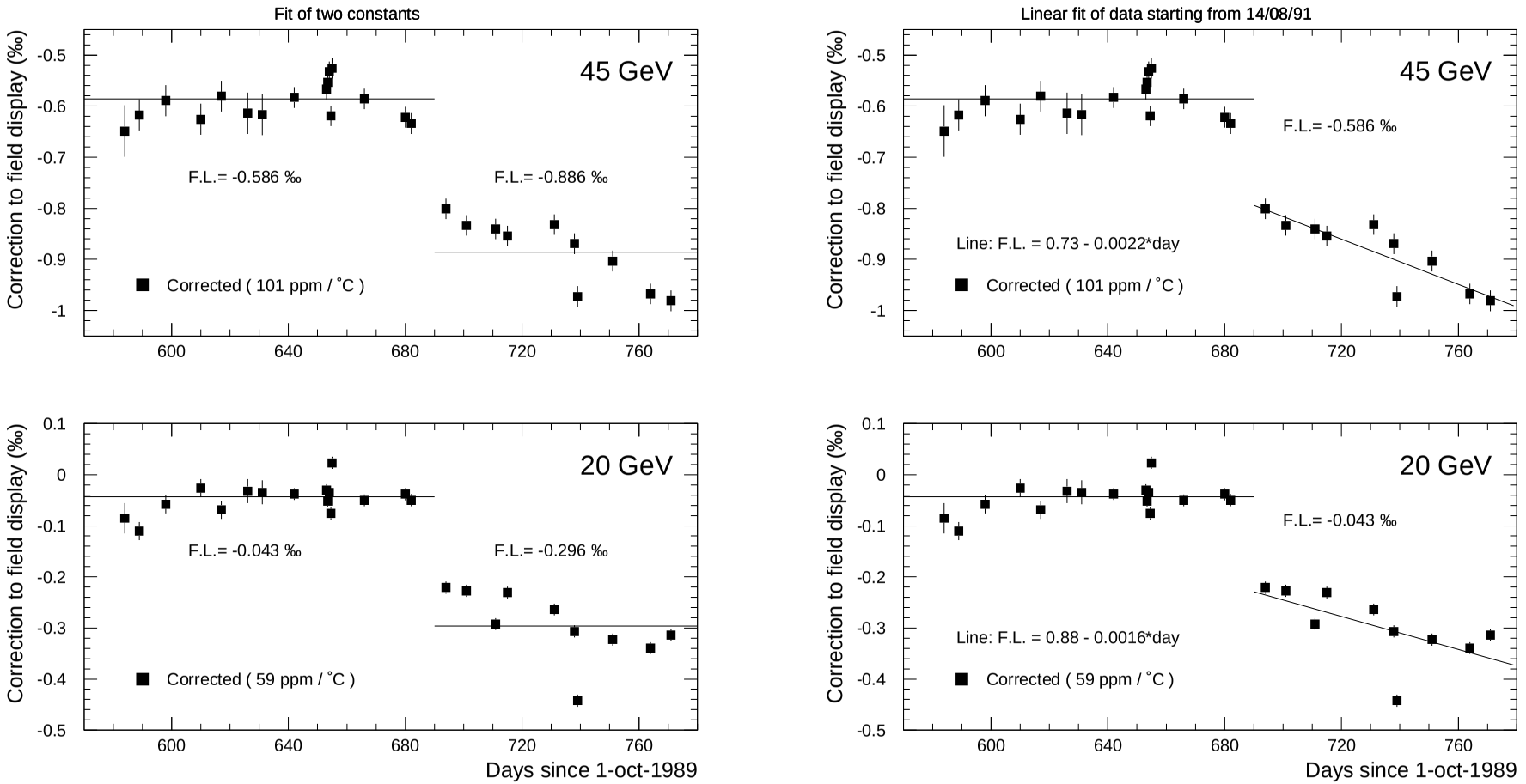

Figure 3: Flux-loop measurements from May to November 1991. The fitted lines are interrupted at 14 August 1991. The different lines after 14 August show the different hypotheses mentioned in the text.

corresponding to the average of the determination in the ring and in the laboratory (eq. 8 and 9), with an error covering both estimates. For the 20 GeV data we use the number measured in the ring (eq. 7), corrected for the elongation effects,

$$\Delta E/E = (0.37 \pm 0.15) \times 10^{-4} \quad \text{per} \quad {}^{o}\text{C} \quad \text{at 20 GeV} \tag{11}$$

The procedure is to use always eq. 10 for the correction of beam energies at 45 GeV, eq. 11 for beam energy corrections at 20 GeV, and eq. 6 and eq. 7 for the internal temperature dependence of flux-loop measurements at 45 and 20 GeV respectively.

As effective temperature measurement we use the average temperature of the eight dipoles, T_8. We choose the reference temperature to be the average during the polarization runs, i.e.

$$\langle T_8 \rangle = 22.25\ {}^{o}\text{C}. \tag{12}$$

The uncertainty in measuring the relative effective temperature is 0.25 ^{o}C and in the determination of the temperature coefficients is 25%.

Measurements of the temperature of the set of eight reference dipoles in the ring were available during the energy scan. For each fill the minimum, maximum and weighted mean temperature was evaluated. The weighting was done according to integrated luminosity. The data are given in Appendix C, and shown in Fig. 4. In summary, the average temperatures observed are:

label	nominal energy [GeV]	average T_8 [^{o}C]	r.m.s. spread [^{o}C]
-3	44.250	22.95	0.6
-2	44.750	22.73	0.6
-1	45.125	23.06	0.4
PEAK	45.625	22.98	0.6
$+1$	46.000	22.94	0.4
$+2$	46.500	22.90	0.6
$+3$	46.875	23.07	0.4

It is concluded that an average temperature of

$$\langle T_8 \rangle_{phys} = 22.96\ {}^{o}\text{C} \ \pm \ 0.25\ {}^{o}\text{C} \tag{13}$$

represents well the data.

Due to the temperature spread of ± 1 ^{o}C, the energy of each fill must be corrected for the temperature dependence; the resulting fill-to-fill error is then given by the 0.25 ^{o}C systematic uncertainty in the temperature definition and the 25% error in the coefficient of the temperature correction, typically in terms of centre-of-mass energy $\Delta E^{temp}_{phys} = \pm 3$ MeV.

2.3 Polarization measurements

By inducing a *controlled spin-depolarizing resonance* on a transversely polarized beam, the mean beam energy can be determined to great accuracy. A frequency-controlled radial RF magnetic field makes the particle spin to precess away from the vertical axis. An artificial depolarizing resonance occurs when the radial magnetic field oscillates at the spin precession frequency, $\omega_{dep} \equiv \omega_s = 2\pi\nu_s\, f_{rev}$. The spin tune ν_s (number of spin precessions per revolution) is related to the beam energy via

$$\nu_s \equiv a_e\, \gamma = \frac{E}{m_e c^2/a_e} = N_s + \delta\nu_s \tag{14}$$

where $a_e \equiv (g-2)/2 = 1.159\,652\,188 \times 10^{-3}$ is the $e^{\pm}$ gyromagnetic anomaly known to a precision of some 10^{-9}, and N_s is the integer part of the tune. A measurement of the depolarizer frequency at the resonance $f^{res}_{dep} = \delta\nu_s \times f_{rev}$ gives the non-integer part, $\delta\nu_s$, of the spin tune and defines the *mean beam energy* in the arcs:

$$E_{beam} = \frac{m_e\, c^2}{a_e}\, \nu_s = 0.4406486\ (N_s + \frac{f^{res}_{dep}}{f_{rev}}) \tag{15}$$

The integer part of the spin tune at the Z energy is $N_s = 103$. From eq. (14) a spin tune sweep of $\Delta\delta\nu_s = \nu_s\, \frac{\Delta E}{E} = 0.01$ corresponds to a relative energy change of $\simeq 10^{-4}$. The method has been adopted to calibrate the LEP beam energy close to the Z-resonance to an accuracy in the order of 10^{-5}, an order of magnitude better than by the other methods.

Transverse electron polarization was observed during eight experiments in 1991 with a level between 5% and 16% [3]. Polarization was observed up to now under special operational conditions, distinct from

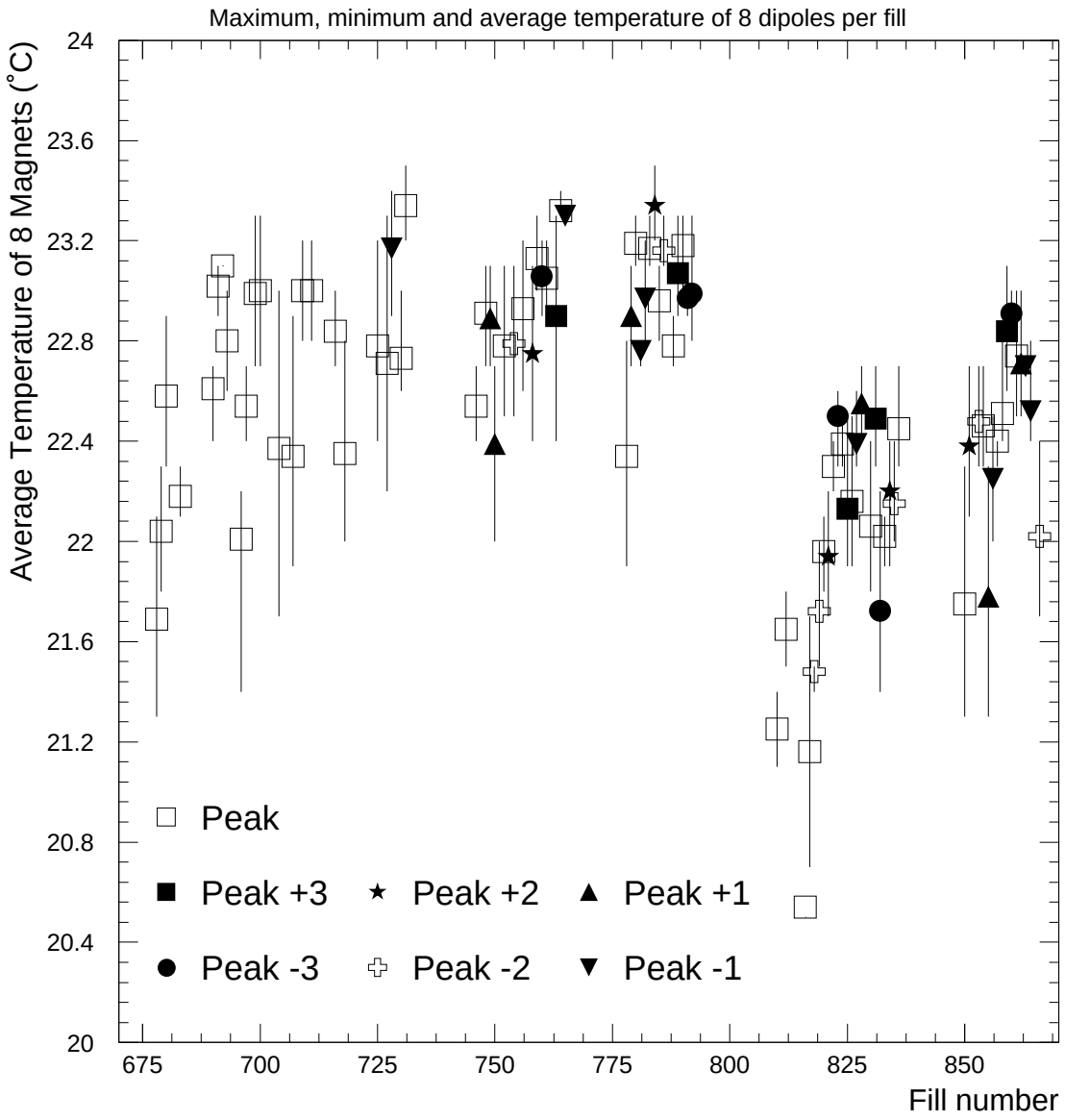

Figure 4: Magnet temperature for each fill since July 1991 when the measurements were available for the set of eight reference dipoles. The symbols give the weighted average temperature, while the extremes of the error bars give the minimum and maximum temperature during the fill.

those of the physics runs (no low beta, solenoids off, one single beam, and a different fractional tune value), and at a single nominal energy setting, 46.5 GeV.

The fact that measurements could be performed at only one energy is a serious limitation, since non-linearities and systematic energy-point-to-energy-point deviations could not yet be checked. In total, six measurements of the beam energy were obtained, resulting in:

$$E_{pol} - E_{FD} = (-34 \pm 3.7) \text{ MeV}; \tag{16}$$

the spread is calculated after temperature correction, which was applied according to eq. 10. The polarization experiments give directly the energy of the beam at the time of measurement, and need no correction, provided there are no systematic effects. Some sources of systematic effects have been checked (β-motion, synchrotron satellites). The "non-linear" ones (energy spread, sextupoles, polarization level) were estimated to be negligible, although further checks will be performed in the future.

Table 3: Resonant-depolarization results in 1991 [3]. The temperature correction is applied according to eq. 10.

Week	37a	37b	40	43	45a	45b
Date	16.9.91	16.9.91	02.10.91	26.10.91	11.11.91	11.11.91
Time	5:00	10:00	5:00	18:00	2:00	7:00
$Q_x - 70.0$	0.136	0.136	0.140	0.137	0.1389	0.1358
$Q_y - 76.0$	0.203	0.203	0.203	0.2014	0.2113	0.2014
Q_s	0.083	0.083	0.083	0.0834	0.083	0.083
Avg. T_8(^{o}C)	22.4	22.6	22.25	22.0	22.1	22.4
E_{FD} (GeV)	46.509 $\pm$0.001	46.509 $\pm$0.001	46.5095 $\pm$0.001	46.508 $\pm$0.001	46.506 $\pm$0.001	46.5065 $\pm$0.001
E_{pol} (GeV)	46.4719 $\pm$0.0006	46.4741 $\pm$0.0006	46.4770 $\pm$0.0006	46.4766 $\pm$0.0006	46.4685 $\pm$0.0013	46.4729 $\pm$0.0005
$E_{pol} - E_{FD}$ (MeV)	-37.1 $\pm$1.2	-34.9 $\pm$1.5	-32.5 $\pm$1.2	-31.4 $\pm$1.2	-37.5 $\pm$1.6	-33.6 $\pm$1.2
Avg. Temp. corr. (MeV)	-0.7	-1.6	0.0	+1.2	+0.7	-0.7
$E_{pol} - E_{FD}$ (T-corr.) (MeV)	-37.8 $\pm$1.2	-36.5 $\pm$1.5	-32.5 $\pm$1.2	-30.4 $\pm$1.2	-36.8 $\pm$1.6	-34.3 $\pm$1.2

The resolution of the resonant-depolarization method is good enough to allow insight into the energy reproducibility of LEP. A spread in the data of ± 3.7 MeV ($\pm 8 \times 10^{-5}$) was observed over the two months testing as well as in the same fill.

The data are given in Table 3. The average temperature T_8 was constant to $\pm 0.21\,^{\circ}C$ during the six polarization measurements so that the E_{pol} data can not disprove the temperature dependence observed with the flux-loop [4].

The temperature correction (last row of Table 3) does not improve the observed spread. It is possible that other effects, such as tidal forces or differences in the settings of corrector magnets are responsible for the variation. Assuming a random sampling of these variations the mean is determined to

$$E_{beam} - E_{FD} = (-34 \pm 1.9) \text{ MeV}, \tag{17}$$

taking into account that four distinct measurements were performed. In terms of centre-of-mass energy:

$$E_{CM} - 2E_{FD} = (-68 \pm 3.7) \text{ MeV}. \tag{18}$$

2.4 Measurements with protons and central radio frequency determinations

2.4.1 Measurements of the circumference of LEP

The magnetic measurements of the beam energy in LEP assume that the particle beams are on the central orbit, i.e. the orbit where the net bending due to quadrupoles and sextupoles vanishes. This central orbit, with average radius R has a revolution frequency f_{ce} and a "central" frequency of the RF system, $f_{RF_{ce}}$,

$$f_{ce} = \frac{\beta_e c}{2\pi R}, \qquad f_{RF_{ce}} = h_e f_{ce} \tag{19}$$

where $h_e = 31324$ is the harmonic number for electrons and positrons. The method used to determine the central orbit relies on the fact that the sextupoles and the quadrupoles are supported by the same girders, on which their relative alignment was precisely adjusted. When the beam goes through the centre of the sextupoles the betatron tunes Q_x and Q_y are independent of the excitation of the sextupoles. The measurements then consist of a precise measurement of the horizontal and vertical tune values for a set of different radio frequencies and sextupole excitation currents. The straight lines fitted to the tune values measured as a function of the frequency of the RF system give the linear chromaticity $dQ/(dp/p)$ for each dipole setting. The frequency, $f_{RF_{ce}}$, corresponding to the central orbit is defined by the intersection of the lines at different chromaticities, since here the orbit is in the magnetic centre of the sextupoles. Due to variations of the current settings during the measurements all line pairs do not exactly intersect at the same point.

A statistical analysis of the data yields an estimate of the uncertainty in the crossing point of 10 to 15 Hz, the later measurements being the more precise ones. Including systematic effects, such as slow tune drifts, a total uncertainty of 20 Hz is estimated. The observed spread in the measurements is consistent with the estimate of the uncertainty. Table 4 summarizes the measurements. The corresponding circumference is (26658.872 ± 0.002) m.

Table 4: Measurements of the central frequency of the RF-system for positrons. For the individual measurements the error bars indicate the spread of the intersections of the straight lines at different chromaticity. In the averages the error bars take into account the spread of the individual data points. Only the last four digits of the frequency are given. Due to the small number of measurements these errors are unreliable estimates of the uncertainties. As discussed in the text the uncertainty is 20 Hz.

Date	11.12.89	21.05.90	28.05.90
energy GeV	20	20	20
from Q_x Hz	..149.4 ± 2.3	..173.0	..164.5 ± 3.4
from Q_y Hz	..156.0 ± 7.6	..178.5	..175.7 ± 4.7
average Hz	..150.9 ± 3.5	175.8 ± 4.5	..169.2 ± 7.9

Measurements at 20 GeV before 1991.

Date	27.05.91	02.09.91	12.09.91
energy GeV	20	20	20
from Q_x Hz	..163.1 ± 2.7	..161.2 ± 8.0	..151.7 ± 2.1
from Q_y Hz	..161.3 ± 2.7	..169.4 ± 22.3	..139.9 ± 29.6
from Q_x Hz	..183.2		..153.3 ± 2.7
from Q_y Hz	..167.3		
average Hz	..168.7 ± 10.0	..163.4 ±11.2	..151.9 ±3.4

Measurements at 20 GeV in 1991.

Date	23.10.91	28.10.91	06.11.91	
energy GeV	46	46	20	46
from Q_x Hz	..175.2 ± 2.6		..169.7 ± 4.3	..145.9 ± 3.2
from Q_y Hz	..185.6 ± 1.6	..201.4 ± 5.3	..174.4 ± 8.2	..177.8 ± 3.2
average Hz	..181.6 ±7.4	..201.4 ± 5.3	..170.5 ± 3.4	..161.9 ± 15.9

Measurements at 46 GeV and at 20 GeV in 1991.

2.4.2 Uncertainty due to non-central orbits

Unlike 1989 and 1990, LEP was run in 1991 with the radio frequency corresponding to the central orbit, $f_{RF} = 352,254,170$ Hz. Therefore, such a correction does not have to be applied to the energy evaluated from magnetic measurements. However, the central frequency has an uncertainty of 20 Hz, and the circumference may be changed by tidal forces as will be discussed below. These effects should be accounted for in the uncertainties when comparisons are made.

The change of momentum for a given change of frequency is given by the momentum compaction

factor, α_c, such that

$$\Delta p/p = -(1/\alpha_c)(\Delta f/f)_{RF} \tag{20}$$

The value of α_c is for the mode of operation in 1991 (and for the earlier data) $\alpha_c = 3.87 \times 10^{-4}$, with an uncertainty of 5 %. For an uncertainty of 10 Hz one obtains $\Delta p/p = 0.7 \times 10^{-4}$, or an uncertainty of $\Delta E_{CM} = 6.8$ MeV at the Z peak.

The frequency of the RF system was kept constant to better than 1 Hz, correspondingly, the non-reproducibility error introduced is smaller than 1 MeV in terms of E_{CM}.

2.4.3 Energy calibration with protons of 20 GeV

The particle momentum corresponding to the central orbit in LEP can be measured at the injection energy using protons [8], [10]. The method is based on the fact that protons at 20 GeV are not yet ultrarelativistic. Their velocity $v_p = \beta_p c$ is therefore different from the speed of light and can be used to determine the momentum.

For the measurements, the *circumference* is determined using the method described above. The velocity of the positrons at 20 GeV is negligibly different from the velocity of light, and can therefore be used to determine the circumference of the machine. The protons are injected into LEP with the same magnetic settings as for positrons and then trapped with the RF-system on a harmonic number, h_p, different from the harmonic number, h_e, of the positrons. The chromaticity can then be measured with protons for different sextupole settings, in the same way as it is done with positrons. This determines the central frequency for protons, $f_{RF_{cp}}$, and the velocity of the protons can be inferred from

$$\beta_p = \frac{h_e f_{RF_{cp}}}{h_p f_{RF_{ce}}} \tag{21}$$

(using $\beta_e = 1$). The harmonic numbers are $h_e = 31324$ and $h_p = 31358$ (at 20 GeV) for electrons and protons respectively. These are known unambiguously, since a change of one unit would correspond to a change of 0.8 m in the circumference.

Measurements with protons were done once in 1989 and 1990, and three times in 1991. Two measurements were performed in September 1991 with a forced temperature difference of 2.8 ^{o}C. The precision of the measurements, however, was not sufficient to determine the temperature coefficient of the magnet strength. The results are summarized in Table 5. Temperature corrections were applied according to eq. 7. Tidal variations may have influenced the measurements (see section 4.2); these are difficult to estimate since the measurements extend over several hours.

3 IP-dependent corrections: RF effects

The circulating electrons and positrons lose about 120 MeV per turn in synchrotron radiation on their curved path through the LEP dipoles. This energy loss is compensated by acceleration in the RF-units, placed left and right of the interaction points 2 (IP2, L3) and 6 (IP6, OPAL). The deviation from the mean beam energy around the ring is illustrated in Fig. 5. Ideally, the sum of e^+ and e^- energies would be constant around the whole ring. In the presence of alignment errors, this is not necessarily the case and corrections on the center-of-mass energies at the collision regions, particularly those close to RF-sections (IP2 and IP6) have to be considered.

The copper cavities in LEP are operated with a sum of two frequencies which produces beating such that the microwave energy oscillates between the acceleration cavities and the storage cavities and overall heat losses are reduced. The alignment has been done for the lower of these two frequencies, leading to a non-negligible misalignment of the cavities for the mean frequency as seen by the beam.

3.1 Energy deviation in the IP

The LEP copper RF system is operated at the two frequencies f_1 and f_2:

$$f_1 = 352.209188\text{MHz and } f_2 = 352.299152\text{MHz} \tag{22}$$

The difference between the two frequencies equals eight times the revolution frequency. The amplitude is the same at the two frequencies. The cavities are aligned for f_1. Therefore, f_2 has a phase error which increases linearly with the cavity distance, d, from the intersection point (IP). The phase error, ϕ_e, written in terms of the distance of the average cavity position from the IP, $d = 197.69$ m, and the frequency difference is

$$\phi_e = \frac{(f_1 - f_2)d}{c} \times 360^o = \frac{-89964 \times 197.69}{299.79 \times 10^6} \times 360^o$$

Table 5: Energy calibration with protons at 20 GeV. We use the notation p_p for the proton momentum, and E_{FD} for the momentum estimate from the field display.

date	11.12.89	21.05.90	27.05.91	02.09.91	12.09.91
day after 01.10.89	71	232	603	701	711
T_8 ^{o}C			23.0 ± 0.5	21.1 ± 0.25	24.1 ± 0.25
average $f_{RF_{ce}}$ Hz	352254150.9 ± 3.5	352254175.8 ± 4.5	352254168.7 ± 10.0	352254163.4 ±11.2	352254151.9 ±3.4
$f_{RF_{cp}}$					
from Q_x Hz	..435.3 ± 19.0	..247.5 ± 19.0	..221.4 ± 89	..149.9 ± 45	..114.0 ± 1.1
from Q_y Hz	..478.7 ± 42.3	..242.6 ± 20	..211.8 ± 34	..132.6 ± 4.8	
from Q_x Hz				..123.7 ± 23	
from Q_y Hz				..154.3 ± 9.8	
average Hz	352249470.8 ± 69.2	352249242.6 ± 18.5	352249214.5 ± 49.2	352249138.5 ± 10.6	352249114.0 ± 1.1
β_p	0.998902476	0.998901758	0.998901698	0.998901498	0.998901461
γ_p	21.3500	21.3430	21.3424	21.3405	21.3401
p_p MeV/c	20 010.1 ± 1.9	20 003.5 ± 0.6	20 003.0 ± 1.5	20 001.2 ±0.6	20 000.8 ± 0.1
E_{FD} MeV/c	20 007.0 ± 1.0	20 009.3 ± 1.0	20 006.4 ± 0.5	20 005.4 ± 0.7	20 005.6 ± 0.9
$p_p - E_{FD}$ MeV/c	3.1 ± 2.9	-5.8 ± 1.6	−3.4 ± 2.0	−4.2 ± 1.3	−4.8 ± 1.0
$p_p - E_{FD}$ at 22.25 ^{o}C MeV/c			−4.0 ± 2.0	−3.3 ± 1.4	−6.2 ± 1.1

The result is an average phase error $\phi_e = -21.4^o$ for f_2.

Because $f_2 > f_1$ the phase error is such that the particles arrive too soon in the cavities before the IP and too late in the cavities after the IP for the higher frequency. Therefore the voltage gain before the IP is higher than the average, and it is lower after the IP. This applies to *both* types of particles. The result is a higher centre-of-mass energy in the intersection regions where RF cavities are installed.

The energy difference per beam can be calculated as follows. On the incoming side the energy gain (ΔE_{in}) is given by

$$\Delta E_{in} = U_1 \sin(\phi_S) + U_2 \sin(\phi_S + \phi_e)$$

On the outgoing side

$$\Delta E_{out} = U_1 \sin(\phi_S) + U_2 \sin(\phi_S - \phi_e)$$

where U_1 and U_2 are the accelerating voltages on each side of the IP at frequencies f_1 and f_2 respectively and ϕ_S is the stable phase angle. Note that the accelerating voltage is the same at the two frequencies, i.e $U_1 = U_2$.

The energy of the beams at the IP is higher than the average energy by an amount approximately given by

$$\Delta E = \frac{\Delta E_{in} - \Delta E_{out}}{2}$$

for symmetrically powered R.F cavities.

An example which illustrates the magnitude of the effect is as follows. For values of $U_1 = U_2 = 27$ MV, $\phi_S = 144.8^o$ and $\phi_e = -21.4^o$, corresponding to a total energy loss per turn of about 120 MeV, we find

$$\begin{aligned} \Delta E_{in} &= 38.10 \quad \text{MeV} \\ \Delta E_{out} &= 22.00 \quad \text{MeV} \end{aligned}$$

and the energy offset, relative to the average energy,

$$\Delta E = 8.05 \text{ MeV}$$

The centre of mass energy is thus 16.1 MeV higher than at the interaction points without RF units.

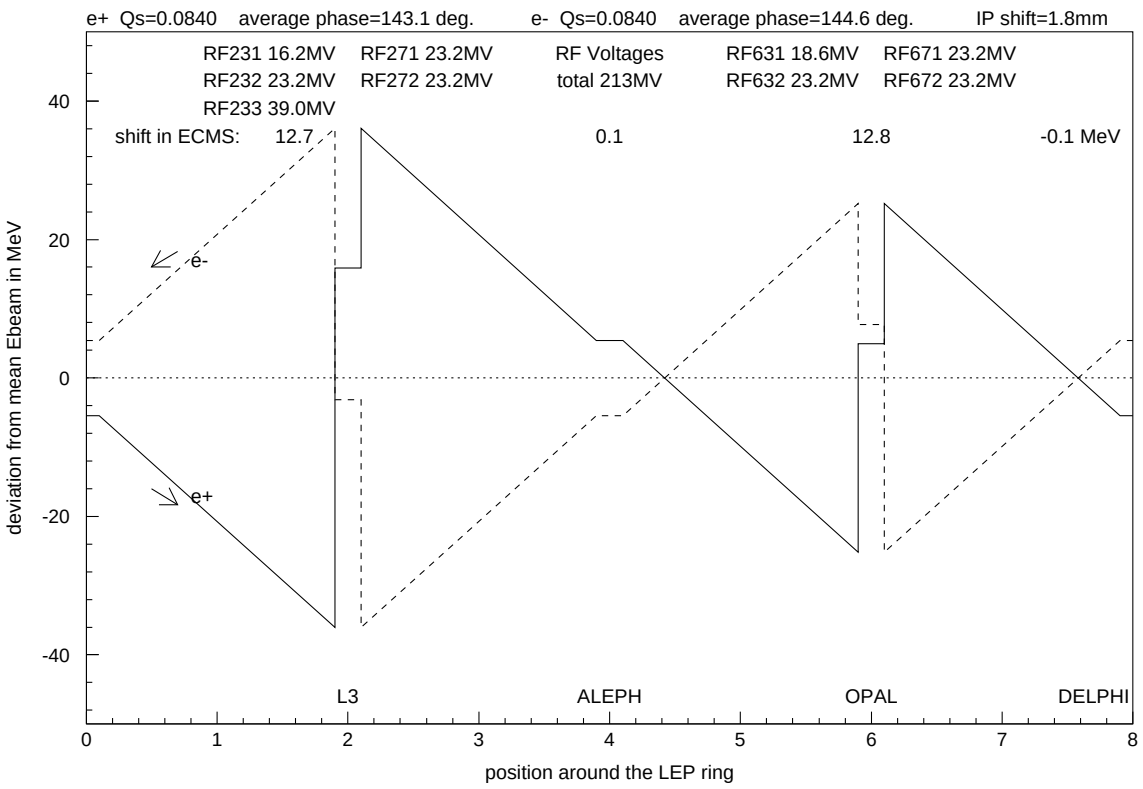

Figure 5: Energy sawtooth plot for the typical RF-distribution during the energy scan 1991.

The exact value of the local energy shift depends on the power distribution in the RF units. In particular, when the super-conducting (SC) RF unit is used, the total power in the copper cavities is lowered, which in turn lowers the local energy shifts in IP 2 and 6, since the SC cavities run at the single frequency f_1. The centre-of-mass energies in IP's 4 and 8 remain unaffected if the power on the cavities on the left-hand side and on the right-hand side of IP 2 and 6 are equal. However, if cavities run at reduced voltages or even trip off, energy changes of the order of 2 MeV occur in *all* interaction points.

3.2 Results of the simulation

The energy corrections for the interaction points as well as their variations with beam energy, the dependence on the voltage distribution on the cavities, the effects of phase tuning errors and of tripping cavities and the Q_S dependence were quantified with simulation programs. If the voltages applied to the cavities are given, then the stable phase angle is determined by the constraint that the energy gain around the ring has to be equal to the energy loss per turn due to synchrotron radiation, $E_{loss} = 122.2$ MeV at 45.6 GeV beam energy. In the simulation, the total voltage was determined from the constraint that the average of the Q_S values of e^+ and e^- is 0.084 (the 1991 average), while the relative contribution of individual cavities to the overall voltage was kept constant. This simulates the procedure used during the energy scan for cavity trips, voltage changes and phase tuning errors. The nominal energy of the beams is defined to be the average energy in the arcs, and all corrections quoted are relative to that. Tables 6 and 7 show the input parameters and the results without and with super-conducting cavities. In the simulation, the geometrical alignment of the cavities was taken to be perfect with respect to f_1, in good agreement with optical survey measurements which show deviations of 1-2 mm only. The phases of the RF voltages on the cavities were assumed to have no error.

The energy corrections in IP 2 and 6 are slightly different due to different voltages on RF units 231 and 631 where cavities were removed to give space to electrostatic separators.

When cavities tripped off during LEP operation, the total voltage on the remaining cavities was increased in order to keep Q_S close to its nominal value; during most of the energy scan this was automatically achieved by software in the LEP control system. The resulting energy changes in the four IP's in cases where cavities are off are shown in Table 8. If the voltages on the copper cavities around an

Table 6: Energy gain of particles in the copper cavities and correction to the energies at the IP's relative to the mean energy in the arcs.

RF unit	distance from IP (in units λ_1)	voltage fraction [%]	energy gain for e^+ [MeV]	energy gain for e^- [MeV]
		total voltage=214.7 MeV		
RF231 (L3 left)	-257.75	9.3	14.7	7.8
RF232 (L3 left)	-203.75	13.3	20.4	12.4
RF271 (L3 right)	260.75	13.3	11.9	20.5
RF272 (L3 right)	203.75	13.3	13.1	19.8
RF631 (OPAL left)	-257.75	10.7	16.9	8.9
RF632 (OPAL left)	-203.75	13.3	20.4	12.3
RF671 (OPAL right)	260.75	13.3	11.8	20.6
RF672 (OPAL right)	203.75	13.3	13.1	19.8
total energy gain			122.2 MeV	122.2 MeV
Q_S			0.084	0.084
ϕ_S			143.1°	144.7°

	normalized energy of e^+ [MeV]	normalized energy of e^- [MeV]	centre-of-mass energy correction [MeV]
IP 2 (L3)	5.14	10.14	15.3
IP 4 (ALEPH)	-0.53	0.28	-0.24
IP 6 (OPAL)	6.2	9.6	15.8
IP 8 (DELPHI)	0.53	-0.28	0.24

Table 7: Energy gain of particles in cavities and correction to the IP energy for the case where the super-conducting cavities are on.

RF unit	distance from IP (in units λ_1)	voltage fraction [%]	energy gain for e^+ [MeV]	energy gain for e^- [MeV]
		total voltage=213.1 MeV		
RF231 (L3 left)	-257.75	7.6	11.9	6.4
RF232 (L3 left)	-203.75	10.9	16.5	10.1
RF271 (L3 right)	260.75	10.9	9.6	16.7
RF272 (L3 right)	203.75	10.9	10.6	16.1
RF631 (OPAL left)	-257.75	8.7	13.6	7.3
RF632 (OPAL left)	-203.75	10.9	16.5	10.1
RF671 (OPAL right)	260.75	10.9	9.5	16.7
RF672 (OPAL right)	203.75	10.9	10.5	16.2
RF233 (L3 SC)	-	18.3	23.4	22.6
total energy gain			122.2 MeV	122.2 MeV
Q_S			0.084	0.084
ϕ_S			143.1°	144.6°

	normalized energy of e^+ [MeV]	normalized energy of e^- [MeV]	centre-of-mass energy correction [MeV]
IP 2 (L3)	15.8	-3.1	12.7
IP 4 (ALEPH)	5.4	-5.4	0.01
IP 6 (OPAL)	5.0	7.8	12.8
IP 8 (DELPHI)	-5.4	5.4	-0.01

IP are not equal, electrons and positrons have a different stable phase angle, ϕ_S^+ and ϕ_S^-, which in turn translates into a shift of the longitudinal position of the interaction point, $\Delta Z = \frac{1}{2}(\phi_S^+ - \phi_S^-) \times \lambda_{RF}/2\pi$. This is also shown in Table 8.

The corrections to the centre-of-mass energies in ALEPH and DELPHI are of equal size but have opposite sign; they are of the same order of magnitude as the changes of the correction to the energies in L3 and OPAL. This should be kept in mind when results from different experiments are combined (the changes in energy scale arising from instabilities of the voltages applied to the copper cavities are anti-

Table 8: Simulation of the effect of cavity trips. The ratios of the voltages on the cavities were chosen according to the values in Table 6 and 7. Shown are the energy changes for all IP's as compared to Table 6 and 7, and the predicted movement of the position of the interaction point relative to its position with all cavities on.

Cavity	ΔE_{CM}^{IP2}	ΔE_{CM}^{IP4}	ΔE_{CM}^{IP6}	ΔE_{CM}^{IP8}	ΔZ [mm]
without super-conducting cavities					
RF231 (L3 left)	-3.0	-2.2	1.4	2.2	-3.1
RF232 (L3 left)	-3.4	-2.8	2.2	2.8	-3.7
RF271 (L3 right)	-3.4	2.8	2.5	-2.8	4.1
RF272 (L3 right)	-2.1	2.2	2.5	-2.2	3.1
RF631 (OPAL left)	1.4	2.4	-3.3	-2.4	-3.6
RF632 (OPAL left)	1.9	2.6	-3.1	-2.6	-3.8
RF671 (OPAL right)	2.4	-2.9	-3.3	2.9	4.1
RF672 (OPAL right)	2.4	-2.3	-2.0	2.3	3.2
with super-conducting cavities					
RF231 (L3 left)	-1.7	-1.3	1.0	1.3	-2.4
RF232 (L3 left)	-1.8	-1.6	1.5	1.6	-2.9
RF271 (L3 right)	-3.6	1.9	1.6	-1.9	3.2
RF272 (L3 right)	-2.5	1.4	1.6	-1.4	2.5
RF631 (OPAL left)	1.8	2.2	-2.7	-2.2	-2.8
RF632 (OPAL left)	2.2	2.4	-2.6	-2.4	-2.9
RF671 (OPAL right)	0.8	-2.6	-2.9	2.6	3.3
RF672 (OPAL right)	1.0	-2.1	-1.9	2.1	2.5

correlated between experiments on opposite sides of the LEP ring). It is also noticeable that the change in energy is correlated with the vertex movements, $|\Delta E|^{av}/|\Delta Z|$ varies between 0.5-0.8 MeV/mm.

The value of Q_S was not kept perfectly constant during the runs. The shifts in energy for the observed variation $0.081 < Q_S < 0.087$ were calculated to be $\Delta E_{CM}^{Q_S} = \pm 1.5$ MeV for IP's 2 and 6 and negligible in IP 4 and 8. Changes of Q_S in combination with cavity trips lead to energy variations in IP 4 and 8 of the order of ± 0.3 MeV; the variations in IP 2 and 6 increase slightly for the IP with the larger energy correction and decrease slightly for the other.

The dependence of this correction in points 2 and 6 on the beam energy was found to be negligible (< 0.5 MeV).

The super-conducting cavities were operated in physics running from fill 825 onwards (see Appendix B). Their average voltage was 41 MV, with a spread of about 7 MV. The energy correction in points 2 and 6 increases by 0.4 MeV if the voltage on the super-conducting cavities is reduced by 5 MV. The observed spread therefore leads to an additional error of ± 0.5 MeV for these periods.

Additional effects arise from deviations of the phase of the RF voltage or its envelope. The typical stability of these phases seems to be around 10° as judged from occasional logbook entries; no periodic measurements are available. These phase errors also lead to differences of the Q_s values of electrons and positrons of the order of 0.001. Different Q_s values of e^+ and e^- were observed in about 20% of the available measurements in physics runs during the 1991 energy scan and could be reproduced by assuming random shifts of the RF phase and the phase of the envelope; a 10° random phase errors on all cavities changed the centre-of-mass energy in all IP's by only about ± 0.5 MeV, accompanied by shifts of the longitudinal position of the interaction point.

Simulation results are summarized in Table 9; the size of the given energy changes will be used below in estimating the systematic uncertainty of the energy scales in each IP.

3.3 Shifts of the longitudinal position of the IP

The size of the predicted shifts is several *mm* (Table 8) and is in principle measurable as a shift of the average longitudinal position of the interaction point in the experiments. The typical integration time needed for the required precision is about one hour under the usual data-taking conditions. These shifts have been observed in coincidence with reported cavity trips with the right amplitude and direction. This yields a strong support for the model used to simulate these effects.

The average position of the interaction points in the four experiments has also been compared and correlated movements of the interaction points were observed. The distribution has a width of about

Table 9: Summary of the simulation results. The variations given here were computed with the super-conducting cavities on. Since the effects scale roughly with the voltage applied to the copper cavities, the variations are $\sim 20\%$ larger when the super-conducting cavities are off.

Source	ΔE_{CM}	
$0.081 < Q_S < 0.087$	± 1.5 MeV	IP's 2 and 6 only
beam energy dependence	$< \pm 0.5$ MeV	IP's 2 and 6 only
SC cavity off/on	$0 \rightarrow (-2.8 \pm 0.5)$ MeV	IP's 2 and 6 only
one Cu cavity off	± 2 MeV *)	all IP's
$\pm 10°$ error on RF phase	± 0.5 MeV	all IP's
$\pm 10°$ error of phase of RF envelope	± 0.5 MeV	all IP's

*) The uncertainty due to random trips is estimated in the following section.

2 mm (rms). Using Tables 6 and 7, one can estimate how often the copper cavities around an IP were powered asymmetrically, either due to cavity trips, voltage changes or phase tuning errors. In fact, as expected, the spread of the vertex shifts becomes smaller by about 25%±10% (stat. error) towards the end of the energy scan, when the super-conducting cavities were on most of the time. Using the worst-case assumption that all vertex movements arise from instabilities of the copper cavities results in an error estimate of ± 1.5 MeV on the centre-of-mass energy.

3.4 Smaller effects

Differences of the path length of the particles in the two arcs - from point 2 to point 6 via point 4 or via point 8 - will lead to energy differences between points 4 and 8. Such differences can be caused either by a geometrical difference of the arc lengths or by different strengths of the bending magnets, which lead to different orbits and therefore different path lengths. The RF phase in cavities at opposite sides of the LEP ring was measured for electrons and positrons. The difference in the path length of the two sides of the LEP ring was measured to be $< \pm 5$ mm, corresponding to an upper limit of ± 1 MeV for this IP-dependent uncertainty.

Twelve of the standard dipoles are replaced by injection dipoles in octants 1 and 8 of LEP. These have half the length and twice the field compared to the standard dipoles and therefore doubled energy loss. The result is symmetric for e^+ and e^- and the correction to the center-of-mass energies is negligible.

3.5 Summary of IP-dependent corrections and their errors

When computing the IP-dependent corrections average values for the voltages on the RF cavities and for Q_s were used and all phases were assumed to be tuned correctly; it is not known how well this represents the average operating conditions of LEP. From the typical spread of these parameters obtained from the available logbook entries and from operating experience it is estimated that the corresponding uncertainties in the centre-of-mass energy should be covered by assigning an overall systematic error of ± 1 MeV to the energies in all interaction points.

In summary, the corrections to be applied to the centre-of-mass energy due to RF effects and their errors are:

without SC RF cavities [MeV]	with SC RF cavities [MeV]
$\Delta E_{CM}^{IP2} = (15.3 \pm 2.3 \pm 1)$	$\Delta E_{CM}^{IP2} = (12.7 \pm 2.3 \pm 1)$
$\Delta E_{CM}^{IP6} = (15.8 \pm 2.3 \pm 1)$	$\Delta E_{CM}^{IP6} = (12.8 \pm 2.3 \pm 1)$
$\Delta E_{CM}^{IP4} = (-0.2 \pm 1.7 \pm 1)$	$\Delta E_{CM}^{IP4} = (0.0 \pm 1.7 \pm 1)$
$\Delta E_{CM}^{IP8} = (0.2 \pm 1.7 \pm 1)$	$\Delta E_{CM}^{IP8} = (0.0 \pm 1.7 \pm 1)$

Note that the energy shifts induced by the variations in the RF power distribution are fully anti-correlated in points 4 and 8 and partially anti-correlated in points 2 and 6. The first error gives the random fill-to-fill uncertainty of the energy corrections, the second one is an overall uncertainty arising from the imperfect knowledge of the average operational parameters of LEP.

4 Other corrections and uncertainties

Some corrections have to be applied making comparisons of similar measurements taken at different times or comparing measurements taken with different methods. Time dependent effects may be induced by temperature differences and by tidal effects or by ageing of some components. Other corrections have

to be applied, e.g. if one compares the results of magnetic measurements with measurements done with beams, the effects of the earth magnetic field cannot be neglected.

4.1 Earth field

The influence of the earth magnetic field changes the effective field seen by the particle beams. The measurements with the flux-loop are not sensitive to the constant additional field, and therefore have to be corrected for it when compared to measurements with beams. The flux-loop measurement results have to be corrected by -1.0 MeV.

4.2 Tidal effects

The tidal forces from the moon and to a smaller extent from the sun, distort the spheroidal shape of the earth. The attraction of these objects produces two symmetric bulges on the surface of the earth. The inclination of the rotational axis of the earth with respect to the plane of the moons orbit introduces an asymmetry in the two daily tides.

The local change of the earth radius induces a small expansion of the solid surfaces of the earth crust ("strain"). The 4.24 km radius of LEP is then expected to change by 0.15 mm. This corresponds effectively to a *central* frequency shift

$$-\Delta f/f \simeq \Delta R/R \simeq \frac{0.15 \times 10^{-3}}{4.24 \times 10^{3}} \simeq 3.5 \times 10^{-8} \tag{23}$$

translating into a 12.5 Hz shift of the effective frequency, and thus, following eq. 20, to an energy change of $\Delta E_{CM} \simeq 8$ MeV from low to high tide.

It has been checked that the six measurements of the beam energy with resonant-depolarization sample the phase of the tidal forces in a representative way. Since this is the case, as shown in Fig. 6, the variations of the polarization measurements include the tidal effects, and provide an estimate of their size. The spread in the polarization data of ± 3 MeV is reduced to ± 1 MeV if one applies a correction according to the correlation observed. This suggests that the tidal effects do play a role, even though the measurements need to be redone in a more systematic way to confirm the effect. It was also checked that the physics runs in the energy scan sample the tidal phases in an unbiased way.

A correction for the tidal variations can only be performed once controlled experiments have been done such that other sources of variation can be eliminated. This has not yet been achieved, and the variations have been accounted for as a source of uncertainty.

4.3 Influence of the corrector dipoles

The settings of corrector magnets change, in principle, the effective bending field seen by the beams. Hence a change of energy is induced for a given circumference dictated by the frequency of the RF-system. The net effect of the corrector fields is, however, not simply applicable as a correction to the total bending field, since some of these correct for misaligned quadrupoles.

It can be argued that only the horizontal correctors in the arcs matter, and their net field is noted regularly during operation of the machine. It is estimated that a fill-to-fill error not larger than ± 3 MeV is induced by the variations in corrector settings. It is assumed that the average net field in the corrector dipoles during polarization calibration runs is not largely different from the situation during physics runs. Assuming a sampling of random fluctuations the uncertainty introduced by an eventual difference is estimated to be ± 1.5 MeV.

5 Comparisons

The magnetic measurements were performed throughout the year and can be compared with the proton measurements at injection energy and with the polarization measurements at the Z pole energy. To make this comparison meaningful, corrections have to be applied for temperature variations (2.2.9), ageing of the flux-loop (2.2.3), the nickel effect (2.2.2) and the earth field (4.1). For the calculations we will use hypothesis I (2.2.8), i.e. constant dipole characteristics during the 1991 scan (see Fig. 3):

$$\begin{array}{ll} \text{at 20 GeV} & \Delta E_{FL}/E = -0.296 \times 10^{-3} \\ \text{at 45 GeV} & \Delta E_{FL}/E = -0.886 \times 10^{-3} \end{array}$$

and assign an error of ± 6 MeV at all energies (equal to 10^{-4} at the full scale of 60 GeV). The effect of using hypothesis II instead of I is a change of -1 MeV at 20 GeV and -3 MeV at 45 GeV.

For comparisons during the period relevant for the energy scan, we use the average of the two proton measurements performed in September, with an error reflecting the spread in the data (Table 5):

$$p_p - E_{FD} = (-4.8 \pm 2) \text{ MeV at 20 GeV} \tag{24}$$

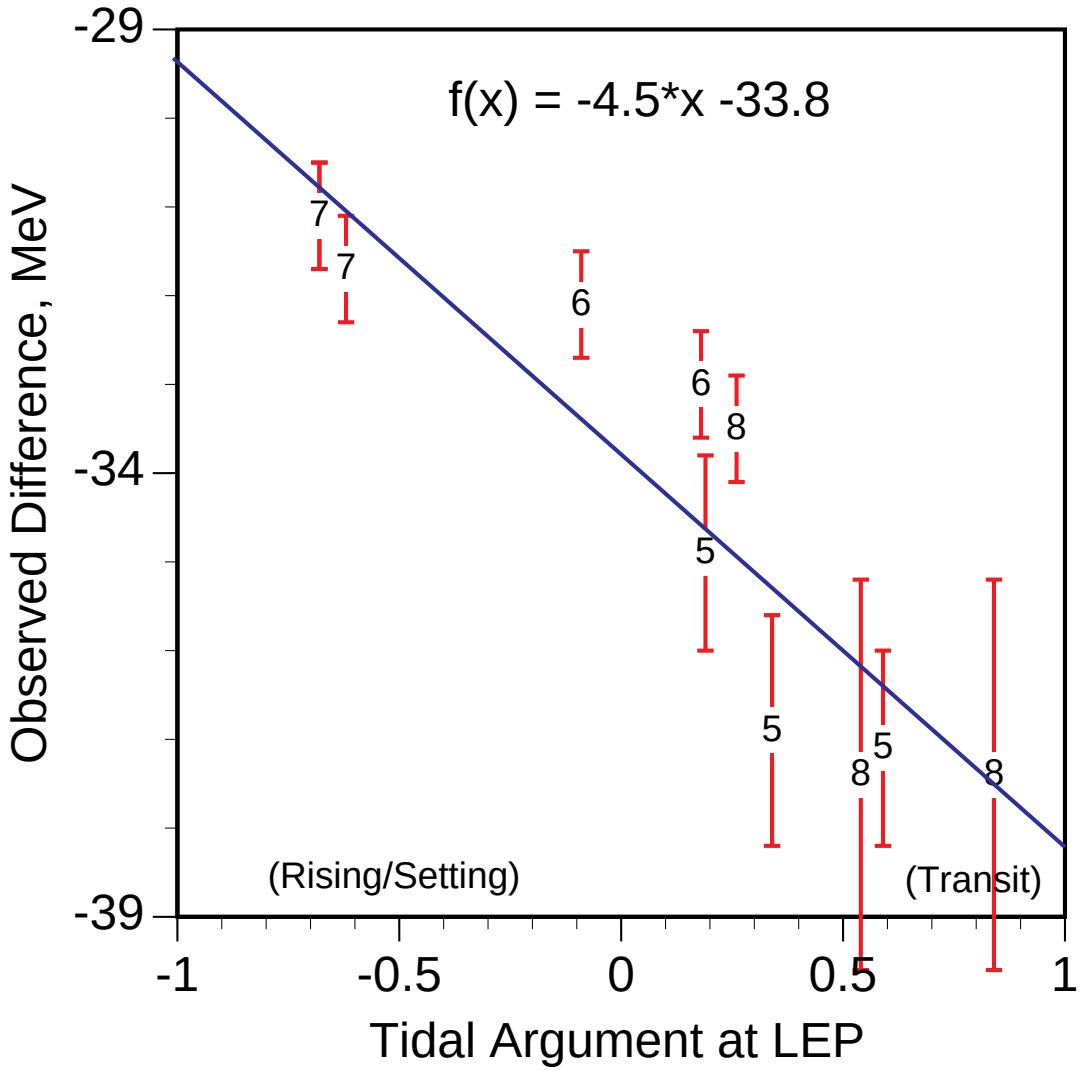

Figure 6: Results of the polarization measurements as a function of the predicted tidal effect of the moon and the sun. The tidal force is plotted on the x-axis with a normalized value between -1 and $+1$ ("tidal argument"). The numbers at the centre of the error bars indicate the numbering of the polarization experiments. (5: week 37; 6: week 40; 7: week 43; 8: week 45.)

The polarization measurements give directly the energy of the beams at the time of measurement (eq. 17), and need no correction. When compared to other measurements, some differences still have to be taken into account, such as the effective temperature, and the fact that the calibrations could only be performed at 46.5 GeV.

The differences between the flux-loop and proton calibrations at 20 GeV corrected to the reference temperature of 22.25^0C, can be calculated as follows:

$E_{FL} - E_{FD}$ (20 GeV)	$-5.9\pm$ 6.0	MeV
Hypothesis I vs II	$\pm$ 1.0	MeV
Temperature corr. error	$\pm$ 1.0	MeV
Nickel effect	$-6.0\pm$ 5.0	MeV
Flux-loop ageing	$+6.0\pm$ 2.0	MeV
Earth field	$-1.0\pm$ 0.0	MeV
Central orbit uncertainty (20 Hz)	$\pm$ 2.8	MeV
Corrected flux-loop (20 GeV)	$-6.9\pm$ 8.7	MeV
$p_p - E_{FD}$	$-4.8\pm$ 2.0	MeV

The two methods of energy calibration give results which are in excellent agreement.

For the comparison at 46.5 GeV the average flux-loop calibration is taken and corrected in the following way.

$E_{FL} - E_{FD}$ (46.5 GeV)	$-41.2\pm$ 6.0	MeV
Hypothesis I vs II	$\pm$ 3.0	MeV
Temperature corr. error	$\pm$ 2.0	MeV
Nickel effect	$-1.0\pm$ 6.0	MeV
Flux-loop ageing	$+13.5\pm$ 4.5	MeV
Earth field	$-1.0\pm$ 0.0	MeV
Central orbit uncertainty	$\pm$ 6.4	MeV
Corrected flux-loop (46.5 GeV)	-29.7 ± 12.1	MeV
$E_{pol} - E_{FD}$	$-34\pm$ 1.9	MeV

The result of the flux-loop is in good agreement with the resonant-depolarization value.

Another comparison can be made by extrapolating the proton calibration at 20 GeV up to 46.5 GeV using the flux-loop data and compare to the polarization result at 46.5 GeV. The high precision of the 20 GeV/c proton calibration is degraded when tracked to 46.5 GeV/c.

$p_p - E_{FD}$ (20 GeV)	$-4.8\pm$ 2.0	MeV
$E_{FL} - E_{FD}$ (20 to 46.5 GeV)	$-35.3\pm$ 6.0	MeV
Hypothesis I vs II	$\pm$ 3.0	MeV
Temperature corr. error	$\pm$ 2.0	MeV
Nickel effect	$+5.0\pm$ 5.0	MeV
Flux-loop ageing	$+7.5\pm$ 2.5	MeV
Earth field	$0.0\pm$ 0.0	MeV
Central orbit uncertainty	$\pm$ 6.4	MeV
Total protons to 46.5 GeV	$-27.6\pm$ 11.2	MeV

The results of the three techniques agree, as can be seen below :

Proton Calibration tracked to 46.5 GeV	-28 $\pm$ 11	MeV
Flux-loop calibration 46.5 GeV	-30 $\pm$ 12	MeV
Polarization	-34 $\pm$ 1.9	MeV

From these comparisons, and in particular the difference of the proton data scaled to 45 GeV and the polarization data, one can estimate the uncertainty in the non-linearities of the energy settings. A change in the calibration constant of 6 ± 12 MeV is observed over a range of 26.5 GeV, or $(0.3\pm0.5)\times10^{-3}$. It cannot be excluded that the trend is higher by a factor two around the Z pole. We assign an uncertainty of $\pm1.5\times10^{-3}$ on the parameter α describing the local scale around $E_{CM} = M_Z$, but this number is largely uncertain (section 2.2.4).

6 Calibration results

For clarity we first discuss the results for the sum of the "average beam energies in the arcs", which is equivalent to the centre-of-mass energy in an interaction point without RF effects. We also take an average temperature and do the calculations at 93.0 GeV to be able to quote a single number. For practical

purposes fill-to-fill temperature dependent corrections and interaction point dependent corrections have to be made. In addition, a local energy-scale correction is needed to obtain the energy for settings different from 93.0 GeV. A table is given in Appendix C to supply this information.

6.1 Absolute calibration of the average beam energy at 93 GeV

The absolute energy calibration is expressed in terms of a correction to be applied to the field display system, which gives for each fill a "measured energy", E_{FD}. The polarization runs were performed at a beam energy of 46.5 GeV (the "+2" setting).

The following components were taken into account for a calibration of the energy:

- The average energy measured with the resonant-depolarization method is taken from eq. 16 with an uncertainty in the mean corresponding to the spread divided by the square root of the effective number of measurements, $\simeq \sqrt{4}$. This gives in terms of centre-of-mass energy (eq. 18)

$$E_{CM}^{pol} - 2E_{FD} = (-68.0 \pm 3.7) \text{ MeV} \tag{25}$$

  where the error stands for the uncertainty in the average value.
- The average temperature during the polarization runs is used as reference point for temperature correction purposes (eq. 12).

$$\langle T_8 \rangle_{ref} = 22.25\ ^{o}\text{C} \tag{26}$$

- A correction for temperature differences is applied using eq. 10:

$$(1.0 \pm 0.25) \times 10^{-4} \text{ per } {}^{o}\text{C}. \tag{27}$$

  Which is the average value of measurements in the ring and in the laboratory.
- Recalling eq. 13, for the physics runs an average temperature of

$$\langle T_8 \rangle_{phys} = 22.96\ ^{o}\text{C}. \tag{28}$$

  has been observed. The uncertainty in relative temperature differences for the conditions during physics runs and during the polarization runs is estimated to be 0.25 ^{o}C . The spread in temperatures for the 1991 runs is in the order of 2 ^{o}C from minimum to maximum (see Appendix D), and is taken into account on a fill-by-fill basis. The polarization measurement has therefore to be corrected by

$$\Delta E_{CM}^{Temp} = (+7 \pm 3) \text{ MeV} \tag{29}$$

  The error accounts for the uncertainty in the temperature measurements ($\pm 0.25\ ^{o}$C $\rightarrow \pm 2$ MeV) and in the coefficient ($\pm 25\% \rightarrow \pm 2$ MeV).
- To account for the little understood flux-loop drift since mid-August and for fill-to-fill fluctuations an additional error of ± 2 MeV in the centre of mass has to be applied. The uncertainties in the average running condition introduced by the variations in the RF system can be expressed as an uncertainty of ± 1 MeV .

Individual corrections for the local situation in the IP's have to be applied according to section 3.5, and the status of the SC RF must have been corrected for. All other uncertainties have been accounted for in the variations observed in the polarization results (e.g. field display reproducibility, corrector magnets, tidal effects etc.)

The net result is a correction, relative to the field display of

$$E_{CM} - 2E_{FD} = (-61 \pm 5.3) \text{ MeV at 93 GeV} \tag{30}$$

Note that the error is about one-quarter of the error on the 1990 calibration (± 22 MeV)

6.2 Calibration of the other energy settings

The correction defined above applies to the energy at which polarization experiments were done, $E_{beam} = 46.5$ GeV. To arrive at a calibration for the other energies one has to scale the additive correction with the nominal energy setting and to apply a local energy-scale correction (section 2.2.4, eq. 4 and 5). This is done in the table below:

label	nominal energy [GeV]	ΔE_{CM} (eq. 30) MeV	ΔE_{CM} local scale corr. MeV
-3	44.250		$-49 \pm 5 \pm 7$
-2	44.750		$-52 \pm 5 \pm 5$
-1	45.125		$-54 \pm 5 \pm 4$
PEAK	45.625		$-56 \pm 5 \pm 3$
$+1$	46.000		$-58 \pm 5 \pm 2$
$+2$	46.500	-61 ± 5	-61 ± 5
$+3$	46.875		$-63 \pm 5 \pm 1$

The last column is the best estimate for the average sum of beam energies for an average situation. The first error is the common energy scale error. The second error accounts for the uncertainty in the local energy-scale correction; these are fully correlated from energy-point to energy-point.

6.3 Non-reproducibility

The polarization measurements provide an estimate of the reproducibility of the beam energy, $\pm 8 \times 10^{-5}$ within the scan data. However, one has to add to this estimate the following effects that do not affect the polarization data, or do affect these data to a lesser extent than the data taken during physics runs. The spread in the polarization data includes tidal effects, field display reproducibility (2.5×10^{-5}), and the influence of corrector magnet settings (3×10^{-5}).

spread in polarization data (includes tidal and other effects)	$\pm 8 \times 10^{-5}$
dipole temperature variations	$\pm 3 \times 10^{-5}$
RF cavity status	$\pm 2 \times 10^{-5}$
total non-reproducibility	$\simeq \pm 10^{-4}$

The error induced by these uncertainties is reduced according to the effective number of fills per energy point.

6.4 Energy-point-to-energy-point errors

In addition to the aforementioned non-reproducibility, systematic effects can change the relative calibration of the various energy-settings used to determine the line-shape. The most natural source of energy-point-to-energy-point errors is non-linearity of the relation between magnetic field seen by the particles in the beam pipe and the predicted field based on the current-settings. Such a non-linearity could either be coming from the magnets themselves or from additional fields that do not scale linearly with magnet current (e.g. the nickel effect and the earth magnetic field). The contribution from the magnets themselves have been measured with the flux-loop and is given in 2.2.4. A precise estimate of the other effects is difficult, the uncertainty has been estimated from the comparison of proton measurements at 20 GeV and polarization data at 45 GeV. As stated in 2.2.4 and 5, we apply a correction of:

$$E_{CM} = 2E_{FD} \left(1 \; + \; \alpha \; \frac{2E_{FD} - 93.0 \text{ GeV}}{2E_{FD}} \right) \tag{31}$$

where $\alpha = (-2.0 \pm 1.5) \times 10^{-3}$, for the 1991 scan data.

A random energy-point-to-energy-point error to account for possible higher order effects in the relation between dipole current and beam energy is estimated as

$$\Delta E_{CM}^{setting}/E = 3 \times 10^{-5} \tag{32}$$

This error could not yet be determined with measurements, and is not precisely known. Since the energy point at 93 GeV was directly measured, this point has no setting error.

6.5 Calibration for data taken in 1991 before 14 August

The change of the cooling system of the LEP dipoles on 14 August 1991, makes it very difficult to trace back the absolute energy scale from the end of 1991 to the data taken before that date, especially since no scan was performed during that time. The energy of the fills were all at the peak value, thus the scale will be defined for this energy only. An average temperature of 22.6 ^{o}C was observed for this period with a rather large uncertainty of 0.5 ^{o}C since no measurements were available before June. The absolute energy will be calculated for this temperature.

It has been decided to define the absolute energy scale of this period by taking the linear average of two methods.

– The absolute calibration of the data during the scan (from the polarization results) corrected for one-half the step observed in the flux-loop measurements. With a step of 3.0×10^{-4} one finds:

$E_{pol} - 2E_{FD}$ scaled to 45.6 GeV at 22.25 ^{o}C	$-68.6\pm$ 6.4	10^{-5}
ΔE_{step}	$+15\pm$ 20.0	10^{-5}
Temperature corr. 22.25 to 22.6 ^{o}C	$+3.5\pm$ 2.3	10^{-5}
Total 1990 prescan at 45.6 GeV at 22.6 ^{o}C	-50.1 ± 21.0	10^{-5}

and hence

$$(\Delta E/E)_{method\ I} = (-50 \pm 21) \times 10^{-5} \text{ at 91.2 GeV and at 22.6 } ^o\text{C} \tag{33}$$

– The second method is the one used in 1990, where the high precision proton calibration is tracked to 45.6 GeV/c with the suitably corrected flux-loop data (obtained from the average of the data before 14 August); an additional uncertainty of ± 6 MeV accounts for the the limited understanding of the flux loop behaviour:

$p_p - E_{FD}$ (20 GeV)	$-4.0\pm$ 2.0	MeV
$E_{FL} - E_{FD}$ (20 to 45.6 GeV)	$-25.8\pm$ 6.0	MeV
flux-loop interpretation	$\pm$ 6.0	MeV
Temperature corr. error	$+1.6\pm$ 2.3	MeV
Nickel effect	$+5.0\pm$ 5.0	MeV
Flux-loop ageing	$+7.5\pm$ 2.5	MeV
Earth field	$0.0\pm$ 0.0	MeV
effect of correctors	$\pm$ 2.0	MeV
uncertainty on RF status	$\pm$ 1.0	MeV
Central orbit uncertainty ($\pm$20 Hz)	$\pm$ 6.4	MeV
Total protons to 45 GeV	-15.7 ± 12.6	MeV

The result is then:

$$(\Delta E/E)_{method\ II} = (-35 \pm 28) \times 10^{-5} \text{ at 91.2 GeV} \tag{34}$$

The results are compatible; the final result is then the average with an error expressing the uncertainty in both methods and the correlation of the errors:

$$(\Delta E/E)^{91\ prescan}_{final} = (-42.5 \pm 20) \times 10^{-5} \text{ at 91.2 GeV and at 22.6 } ^o\text{C} \tag{35}$$

This result has to be corrected for IP-dependent effects and for the fill-dependent magnet temperatures. These corrections have been performed in the table supplied in Appendix C. At the reference temperature of 22.25 ^{o}C we find

$$(\Delta E/E)^{91\ prescan}_{ref} = (-46 \pm 20) \times 10^{-5} \text{ at 91.2 GeV and at 22.25 } ^o\text{C} \tag{36}$$

6.6 Calibration for data taken in 1990

Much less is known of the energy calibration in 1990 than in the 1991 scan. It is recommended to use the 1990 Z mass to recalibrate the 1990 beam energy. This should take care of the (many) things that were not known in 1990 and are known now, such as RF dephasing and absolute energy scale from resonant-depolarization. All the energies given in 1990 can then be rescaled in such a way that the 1990 and 1991 masses coincide. This introduces, on top of the systematic energy scale error, a statistical error in the energy calibration. This statistical error improves when the results of more then one experiment are averaged. This procedure will provide the most reliable estimate of the energy scale, providing no independent measurement of the mass. A local energy scale correction has to be applied as given in eq. 38.

The method of energy calibration used in the past can be updated to reflect the new knowledge gained in 1991. Corrections have to be applied to the flux-loop data (temperature dependence), a correction for the nickel has to be used (new analysis), the IP-dependent effects have to be taken into account, and the non-linearity of the energy scale.

The flux-loop number for the scaling to 45.6 GeV is evaluated from the temperature corrected data starting in May 1990. It is assumed that the average temperature is equal to the 1991 prescan period, i.e. 22.6 ^{o}C. The average of the four flux-loop measurements performed during the physics period for which temperature estimates are available is taken. The "central orbit" correction takes into account that the RF was run at a frequency of (47.1 ± 20) Hz above the central frequency, where the error expresses the uncertainty in the central frequency. The result is obtained as shown in the table:

$p_p - E_{FD}$ (20 GeV)	$-5.8\pm$ 2.0	MeV
$E_{FL} - E_{FD}$ (20 to 45.6 GeV)	$-25.4\pm$ 6.0	MeV
flux-loop interpretation	$\pm$ 6.0	MeV
Temperature corr. to $(22.6 \pm 1.0)\ ^{o}$C	$+1.6\pm$ 4.0	MeV
Nickel effect	$+5.0\pm$ 5.0	MeV
Flux-loop ageing	$+7.5\pm$ 2.5	MeV
Earth field	$0.0\pm$ 0.0	MeV
effect of correctors	$\pm$ 2.0	MeV
Central orbit correction	$-15.8\pm$ 6.4	MeV
Uncertainty in IP-dependent correction	$\pm$ 2.0	MeV
Total protons to 45 GeV	-32.9 ± 13.0	MeV

The result is then:

$$(\Delta E/E)_{1990\ method} = (-72 \pm 29) \times 10^{-5} \text{ at } 45.6 \text{ GeV and at } 22.6\ ^{o}\text{C}, \tag{37}$$

in agreement with the result obtained in 1990 [9].

To this value the IP-dependent corrections have to be added, as given in section 3.5, for the case without SC RF cavities. The uncertainties in the RF status are larger by a factor two compared to the 1991 data due to a higher frequency of RF-trips. The numbers are given in the following table; the first error is a random fill-to-fill uncertainty, while the second error reflects the uncertainty in the average RF status, and is a scale uncertainty already taken into account in eq. 37.

1990 IP-dependent correction
$\Delta E_{CM}^{IP2} = (16.0 \pm 4.5 \pm 2)$ MeV
$\Delta E_{CM}^{IP6} = (16.0 \pm 4.5 \pm 2)$ MeV
$\Delta E_{CM}^{IP4} = (0.0 \pm 3.5 \pm 2)$ MeV
$\Delta E_{CM}^{IP8} = (0.0 \pm 3.5 \pm 2)$ MeV

It is clear that no new information on the mass can be obtained from this calibration, since the systematic errors in the energy scale are 50% correlated with the ones in 1991, and large additional uncertainties are present.

The measurement of the width has to be corrected for the local energy scale. As stated in section 2.2.4, we apply a correction of:

$$E_{CM} = 2E_{FD}\left(1 \ + \ \alpha \ \frac{2E_{FD} - 91.2 \text{ GeV}}{2E_{FD}}\right) \tag{38}$$

where $\alpha = (-2.0 \pm 1.5) \times 10^{-3}$, for the 1990 data.

6.7 Energy spread

At the central energy E_c=45.6 GeV the relative rms. energy spread is $\sigma_E/E = 0.716 \times 10^{-3}$. For different energies this number scales linearly with energy. The error on this number is mainly given by variation of the central frequency of the RF-system for which the beam goes through the center of the quadrupoles. This frequency showed variations of up to 20 Hz while the applied radio frequency stayed constant. The resulting change of the energy spread is about 2.5 %. The absolute spread of the center-of-mass energy is $\sigma_{CM} = \sqrt{2}\sigma_E \approx 46$ MeV. This is only correct if the colliding electrons and positrons have arbitrary energy distributions. For a finite dispersion in the interaction point positrons with an excess energy tend to meet electrons with excess energy. We estimated that the corrected center of mass energy spread is about $\sigma_{CM} \approx 1.55\sigma_E \approx$ 51 MeV with an error of about 5 MeV.

6.8 Treatment of the corrections

The LEP energies are given per fill and per experiment in Appendix C. The energy for fill f of the energy scan point i will be denoted E_f^i. These energies are obtained from the field display readings, to which the following corrections are applied:

- Overall energy scale, determined from the resonant-depolarization runs at $E_{CM} = 93$ GeV, $\left(\frac{\Delta E}{E}\right)_{abs} = -(73.0 \pm 5.7) \times 10^{-5}$, where the error combines the uncertainties from the polarization measurements, the temperature corrections, the average running condition of the RF system and the error introduced by the little understood flux-loop drift (eq. 30). The absolute value is taken from eq. 18.
- A local scale correction of $\alpha = (-2.0 \pm 1.5) \times 10^{-3}$ (eq. 31).

- A temperature correction based on the readings of thermometers situated on top of eight magnets around the ring, T^i_{8f}. The energies are corrected to the average temperature recorded during the polarization runs , $\langle T_8 \rangle = 22.25\ ^\circ C$, taking into account the temperature coefficient $C_T = (1.0 \pm 0.25) \times 10^{-4}\ /^\circ C$.
- An IP-dependent correction, $\delta_{RF}(IP)$, estimating the effect of the particular phasing of the RF cavities, possibly taking into account the status of the LEP RF during that particular fill.

The full set of corrections is included in the formula:

$$E^i_f = 2E^i_{f\,FD}\left[1 + \left(\frac{\Delta E}{E}\right)_{abs} + \alpha\ \frac{(2E^i_{f\,FD} - 93.0\ \mathrm{GeV})}{2E^i_{f\,FD}} + C_T(T^i_{8f} - \langle T_8 \rangle_{Pol}) + \delta_{RF}(IP)\right] \tag{39}$$

6.9 Treatment of the errors

The energies given can be used to fit the line shape and asymmetries to obtain the values of the Z parameters, and their statistical and experimental systematic errors. The errors related to LEP energy systematics have to be calculated as well. In order to do so, it is convenient to describe the errors as originating from the following uncorrelated sources:

- Absolute energy scale, $\left(\frac{\Delta E}{E}\right)_{abs} = 5.7 \times 10^{-5}$.
- Local energy-scale error $\Delta\alpha = 1.5 \times 10^{-3}$.
- Energy-point-to-energy-point errors that account for possible higher order effects in the relation between dipole current and beam energy, $\left(\frac{\Delta E}{E}\right)^{setting}_{p-t-p} = 3\ \times\ 10^{-5}$, except at $E_{CM} = 93$ GeV.
- Non-reproducibility errors $\left(\frac{\Delta E}{E}\right)_{rep} =\ 10^{-4}$ which account for uncertainties in the exact meaning of the temperature readings and the variability thereof, fluctuations due to tidal effects, corrector settings and unknown variations in the RF status; these errors are relevant to each fill. However, in the fitting process it is adequate to group data taken at energies that are nominally the same or very close to each other into "scan points". Therefore one can assume that this error, uncorrelated from fill to fill, is reduced by the number N^i_{fills} of fills at each scan point i. In fact, since the integrated luminosity per fill $\mathcal{L}_f$ is not constant, it is more rigorous to introduce the *effective* number of fills,

$$\overline{N}^i_{fills} = \frac{\left(\sum_{fills} \mathcal{L}_f\right)^2}{\sum_{fills} \mathcal{L}_f^2}$$

  This number is 4 for most practical purposes.
- The last two errors can be summed into one energy-point-to-energy-point error:

$$\left(\frac{\Delta E}{E}\right)^i_{p-t-p} = \sqrt{\left(\frac{\Delta E}{E}\right)^{setting^2}_{p-t-p} + \frac{1}{\overline{N}^i_{fills}}\left(\frac{\Delta E}{E}\right)^2_{rep}}, \tag{40}$$

  which represents seven independent error sources for the seven energies of the scan.

One can define nine random variables X with zero mean and unit variance. The fluctuations of each energy point around the luminosity weighted mean of its various fills is then:

$$\frac{\Delta E^i}{E^i} = \left(\frac{\Delta E}{E}\right)_{abs} \times X_{abs} + \frac{(E^i - 93)}{E^i}\Delta\alpha \times X_\alpha + \left(\frac{\Delta E}{E}\right)^i_{p-t-p} \times X^i \tag{41}$$

One can use the above equation to calculate the correlation between the fit parameters and the correlation matrix between the various scan points.

An analysis of the error sources of the 1990 and 1991 energy calibration shows that only part of the 1991 errors are independent of the errors in 1990, namely the error related to the polarization calibration. This uncorrelated error is negligible compared to the uncertainty in the 1990 data. Hence, the absolute scale for the data taken before the scan in 1991 cannot be used to improve the combined systematic error, it follows then that

$$\sigma(1990 + 1991)_{syst} = \sigma(1991\ scan)_{syst} \tag{42}$$

7 Conclusion

The numbers in this section are given as illustration only. The exact numbers will be determined by the fit to the line-shape performed by each experiment.

The resulting correction to the absolute calibration at 45.625 GeV is directly related to the measurement of the mass of the Z. The result is a correction, relative to the field display of

$$\sigma(M_Z)_{syst} = \left[\begin{array}{c} -40.7(-43.3) \\ -56.2(-56) \\ -40.2(-43.2) \\ -55.8(-56) \end{array} \right] \pm \ 6.3 \text{ MeV} \tag{43}$$

The numbers outside (inside) parentheses give the correction when the SC RF was off (on). The rows give the values for IP 2, 4, 6, and 8, respectively. The error is estimated from the scale and fill-to-fill uncertainties, for a typical number of fills analysed, but can vary slightly from experiment to experiment depending on the data sample used.

The uncertainty in Γ_Z has terms corresponding to the local energy-scale, absolute calibration, fill-to-fill reproducibility, and energy-point-to-energy-point uncertainty.

$$\sigma(\Gamma_Z) = \Gamma_Z \left(\frac{\Delta E}{E}\right)_{local} \oplus \ \Gamma_Z \left(\frac{\Delta E}{E}\right)_{abs} \oplus \ 0.6 \times M(\mathrm{Z}) \left(\frac{\Delta E}{E}\right)_{rep} \frac{1}{\sqrt{n-1}} \ \oplus \\ 0.6 \times M(\mathrm{Z}) \left(\frac{\Delta E}{E}\right)_{p-t-p} \tag{44}$$

where $\oplus$ stands for summing in quadrature, and n is the number of scans ($n = 5$). The statistical factor 0.6 follows from the fitting procedure with the predicted shape of the Z-peak. For the values we use

	value (10^{-3})	contribution to Γ_Z (10^{-3})
$(\Delta E/E)_{local}$	1.5	1.5
$(\Delta E/E)_{abs}$	0.15	–
$(\Delta E/E)_{rep}$	0.1	1.1
$(\Delta E/E)_{p-t-p}$	0.03	0.66

This results in an uncertainty in the width of

$$\sigma(\Gamma_Z) = \pm 4.9 \text{ MeV} \tag{45}$$

using $\Gamma_Z \simeq 2.5$ GeV. It should be noted that the main components in the uncertainties in the width are difficult to estimate, and a certain arbitrariness persists in these numbers.

The contribution to the error in the forward backward asymmetry at the peak is dominated by the uncertainty of the energy before 14 August 1991. With a value of 2×10^{-4} for this scale uncertainty and keeping in mind that one-half of the statistics at the peak were obtained before that time we find:

$$\sigma(A_{FB}^{peak}) = \pm 0.0008 \tag{46}$$

The result of the 1991 energy calibration is a factor four more precise than the values obtained before. This is mainly due to the availability of the resonant-depolarization technique to determine the absolute energy scale. The full power of this technique has not yet been explored. In particular, the uncertainties in the width can be greatly reduced by a measurement at two different energy points, suitably chosen above and below the peak, e.g. at the "+2" and "−2" point. The addition of more well-calibrated energy points can still reduce the width uncertainty. Also in the mass, the understanding of tidal effects and a better control and understanding of temperature effects can provide a significant improvement over the existing data. These issues also rely on precise polarization measurements.

References

[1] D. Decamp et al., (ALEPH Coll.) Z. Phys. C53 (1992) p. 1;
P. Aarnio et al., (DELPHI Coll.), Nucl. Phys. B367 (1991) p. 511;
B. Adeva et al. (L3 Coll.), Z. Phys. C51 (1991) p. 179;
G. Alexander et al. (OPAL Coll.), Z. Phys. C52 (1991) p. 175;
(The LEP collaborations) Phys. Lett. B276 (1992) p. 247.

[2] L. Knudsen *et al*, "First Observation of Tranverse Beam Polarization in LEP", Phys. Lett. B270 (1991) p. 97.

[3] L. Arnaudon *et al*, "Measurement of LEP Beam Energy by Resonant Spin Depolarization", CERN-PPE/92-49, CERN-SL/92-16(AP), subm. to Phys. Lett. B.

[4] J. Gascon *et al*, "The temperature dependence of the energy calibration of LEP beams by flux loop measurements", LEP Performance Note 74, CERN, 1991.

[5] G. Fischer, "Ground Motion – An Introduction for Accelerator Builders", SLAC-PUB-5756 (February 1992), Invited talk at the CERN Accelerator School, March 1992, Montreux, Switzerland.

[6] J. Billan, J.P. Gourber, K.N. Henrichsen and L. W. Walckiers, "Field Display System for the Forecast of Beam Momentum and Betatron Frequencies at LEP", XIV Int. Conf. on High Energy Accel., Tsukuba, Japan, August 1989.

[7] J. Billan, J.P. Gourber and K.N. Henrichsen, "Determination of the particle momentum in LEP from precise magnet measurements", 1991 Particle Accelerator Conference, San Francisco, CA, May 1991.

[8] R. Bailey *et al*, "LEP Energy Calibration", 2nd European Particle Accelerator Conference, Nice, France, June 1990 (CERN SL/90-95).

[9] V. Hatton *et al*, Working group on LEP Absolute Energy, "LEP Absolute Energy in 1990", LEP performance Note 12, CERN, 1990.

[10] A. Hofmann, and T. Risselada, LEP Note 383, 1982.

A Results of flux-loop measurements

This table summarizes all flux-loop measurements performed. For the data before July 1991 the temperature is estimated. Diff is the correction to be applied to the field display readings; T_8 is the temperature of a reference set of eight magnets.

			uncorrected			temp.-corrected c)		
Date	Time	days since 1/10/89	diff [o/oo] 20 GeV	diff [o/oo] 45 GeV	T_8 ^{0}C	diff [o/oo] 20 GeV	diff [o/oo] 45 GeV	diff [MeV] 20-45
04 10 89	a)	3.0	0.484	0.556	*a)*			
08 11 89	00 30	38.0	−0.157	−0.155	20.4 ± 0.5	−0.048	0.032	2.4
21 11 89	13 15	51.0	−0.200	0.019	23.1 ± 0.3	−0.250	−0.067	2.0
28 11 89	04 00	58.0	0.215	−0.080	20.6 ± 0.5	0.312	0.087	−2.3
05 12 89	a)	65.0	0.302	0.081	*a)*			
19 12 89	14 00	79.0	0.222	−0.180	20.8 ± 0.4	0.308	−0.034	−7.7
13 02 90	b)	135.0	−0.139	−0.613	20.0 ± 1.0	−0.006	−0.386	−17.2
07 04 90	04 45	188.0	−0.155	−0.673	20.5 ± 1.0	−0.052	−0.496	−21.3
25 04 90	a)	206.0	0.006	−0.597	*a)*			
16 05 90	a)	227.0	−0.129	−0.727	*a)*			
19 06 90	b)	261.0	−0.129	−0.794	20.0 ± 1.0	0.004	−0.567	−25.6
28 07 90	00 00	300.0	−0.175	−0.789	20.9 ± 0.6	−0.095	−0.653	−27.5
30 08 90	00 00	333.0	0.033	−0.495	23.2 ± 0.4	−0.023	−0.591	−26.1
08 04 91	07 15	554.0	−0.207	−0.880	20.9 ± 0.8	−0.127	−0.744	−30.9
22 04 91	08 30	568.0	−0.192	−0.878	22.0 ± 0.5	−0.177	−0.853	−34.8
08 05 91	05 45	584.0	−0.100	−0.674	22.0 ± 0.5	−0.085	−0.649	−27.5
13 05 91	12 30	589.0	−0.037	−0.491	23.5 ± 0.3	−0.111	−0.617	−25.6
22 05 91	13 30	598.0	−0.043	−0.564	22.5 ± 0.3	−0.058	−0.589	−25.4
03 06 91	11 45	610.0	0.018	−0.550	23.0 ± 0.3	−0.026	−0.626	−27.6
10 06 91	11 08	617.0	−0.036	−0.525	22.8 ± 0.3	−0.068	−0.581	−24.8
19 06 91	13 37	626.0	0.018	−0.528	23.1 ± 0.4	−0.032	−0.614	−27.0
24 06 91	11 03	631.0	−0.008	−0.571	22.7 ± 0.4	−0.035	−0.616	−27.0
05 07 91	14 24	642.0	−0.265	−0.972	18.4 ± 0.2	−0.038	−0.583	−25.5
16 07 91	13 01	653.0	0.008	−0.501	22.9 ± 0.2	−0.030	−0.567	−24.9
16 07 91	20 09	653.5	−0.061	−0.569	22.1 ± 0.2	−0.052	−0.554	−23.9
17 07 91	09 01	654.0	−0.120	−0.679	20.8 ± 0.2	−0.034	−0.533	−23.3
17 07 91	18 48	654.5	−0.197	−0.826	20.2 ± 0.2	−0.076	−0.619	−26.3
18 07 91	08 17	655.0	−0.015	−0.591	21.6 ± 0.2	0.023	−0.525	−24.1
29 07 91	10 25	666.0	−0.012	−0.520	22.9 ± 0.2	−0.050	−0.586	−25.3
12 08 91	15 12	680.0	−0.047	−0.637	22.1 ± 0.2	−0.038	−0.622	−27.2
14 08 91	19 06	682.0	−0.171	−0.841	20.2 ± 0.2	−0.050	−0.634	−27.5
26 08 91	11 27	694.0	−0.165	−0.705	23.2 ± 0.2	−0.221	−0.801	−31.6
02 09 91	21 44	701.0	−0.313	−0.980	20.8 ± 0.2	−0.227	−0.834	−33.0
12 09 91	21 51	711.0	−0.201	−0.684	23.8 ± 0.2	−0.292	−0.841	−32.0
16 09 91	10 52	715.0	−0.210	−0.819	22.6 ± 0.2	−0.231	−0.854	−33.8
02 10 91	07 33	731.0	−0.261	−0.827	22.3 ± 0.2	−0.264	−0.832	−32.2
09 10 91	21 18	738.0	−0.475	−1.157	19.4 ± 0.2	−0.307	−0.869	−33.0
10 10 91	10 26	739.0	−0.516	−1.099	21.0 ± 0.2	−0.442	−0.973	−34.9
22 10 91	05 16	751.0	−0.308	−0.878	22.5 ± 0.2	−0.323	−0.903	−34.2
04 11 91	10 52	764.0	−0.301	−0.902	22.9 ± 0.2	−0.339	−0.968	−36.8
11 11 91	09 58	771.0	−0.317	−0.986	22.2 ± 0.2	−0.314	−0.981	−37.9

a) Not available

b) Actual time not available. The flux loop measurement being done at the very beginning of a startup after a long shutdown, the magnets were certainly cold.

c) Flux loop measurements extrapolated to a temperature of 22.25 °C, using temperature coefficients of 101 ppm/°C at 45 GeV and 59 ppm/°C at 20 GeV.

B Status of SC RF in 1991

This table gives the status of the superconducting RF units for fills starting at number 810; for the fills before that time the SC RF was not on during the physics coasts, or only for negligibly short periods. The data are given in pairs of fill number and voltage on the SC cavities in MV (the typical precision is 2 MV).

fill	Voltage	fill	Voltage	fill	Voltage	fill	Voltage
810	40.0	817	40.0	825	42.	826	41.
827	39.	828	41.	830	40.5	831	45.
831	42.5	831	52.5	831	48.5	831	46.5
831	45.	832	41.	832	45.	832	41.
833	40.	834	42.	835	39.	836	41.
850	40.	851	41.5	853	42.	853	45.
853	42.	854	40.5	855	40.	856	41.
856	46.	856	43.5	856	42.5	856	44.
857	41.0	857	43.5	857	42.25	857	41.5
858	41.0	859	45.0	859	47.5	859	21.0
859	21.5	859	23.0	860	43.5	861	40.0
862	46.0	862	47.5	862	48.5	863	47.5
864	40.	864	42.	866	17.5	866	20.

C Physics fill data

Best estimate of the energy of each physics fill in 1991 for the four IP's. Column 1: fill number, Column 2: energy point in the scan, Column 3: average field display energy during the fill, Columns 4-7: best estimate of the centre-of-mass, energy in the four interaction points, Column 8: length of fill in hours, Column 9: estimated integrated luminosty in $mA^2\times$ hours, Column 10: Mean temperature.

Fill Number	Fill Type	E_{FD}	E_{CM}				Fill Length Hours	Int. Lumi	Mean Temp ^{0}C
			IP2	IP4	IP6	IP8			
		[GeV]	[GeV]	[GeV]	[GeV]	[GeV]			
537	0	45.641	91.258	91.243	91.259	91.243	3.7	2.2	22.66
539	0	45.643	91.262	91.247	91.263	91.247	1.7	1.4	22.66
540	0	45.640	91.256	91.241	91.257	91.241	5.5	3.3	22.66
541	0	45.641	91.258	91.243	91.259	91.243	4.4	1.9	22.66
543	0	45.643	91.262	91.247	91.263	91.247	4.3	2.1	22.66
544	0	45.641	91.258	91.243	91.259	91.243	1.2	0.3	22.66
545	0	45.642	91.260	91.245	91.261	91.245	4.5	1.5	22.66
546	0	45.641	91.258	91.243	91.259	91.243	0.3	0.3	22.66
547	0	45.642	91.260	91.245	91.261	91.245	0.2	0.0	22.66
563	0	45.641	91.259	91.243	91.259	91.244	4.8	0.7	22.66
565	0	45.641	91.258	91.243	91.259	91.243	12.6	4.7	22.66
566	0	45.641	91.258	91.243	91.259	91.243	4.6	3.9	22.66
567	0	45.641	91.258	91.243	91.259	91.243	13.4	8.2	22.66
568	0	45.641	91.258	91.243	91.259	91.243	14.9	12.1	22.66
571	0	45.641	91.259	91.244	91.260	91.244	15.6	20.5	22.66
572	0	45.641	91.259	91.243	91.259	91.244	17.5	18.3	22.66
573	0	45.641	91.259	91.244	91.260	91.244	6.1	8.2	22.66
579	0	45.637	91.249	91.234	91.250	91.234	2.5	2.6	22.66
580	0	45.637	91.250	91.235	91.251	91.235	10.5	13.1	22.66
581	0	45.637	91.251	91.235	91.251	91.235	2.3	3.0	22.66
583	0	45.638	91.253	91.237	91.253	91.238	6.0	6.8	22.66
584	0	45.638	91.253	91.237	91.253	91.238	7.2	11.4	22.66
585	0	45.638	91.253	91.238	91.254	91.238	7.9	10.3	22.66
586	0	45.639	91.254	91.239	91.255	91.239	13.0	10.6	22.66
587	0	45.638	91.253	91.237	91.253	91.238	7.5	11.0	22.66
588	0	45.639	91.254	91.239	91.255	91.239	8.2	11.9	22.66
591	0	45.638	91.252	91.237	91.253	91.237	0.3	0.4	22.66
597	0	45.639	91.254	91.239	91.255	91.239	0.5	0.3	22.66
598	0	45.640	91.256	91.241	91.257	91.241	6.1	6.6	22.66
600	0	45.640	91.256	91.241	91.257	91.241	0.8	2.6	22.66
601	0	45.640	91.256	91.240	91.256	91.241	17.3	23.2	22.66
602	0	45.640	91.257	91.242	91.258	91.242	3.6	8.7	22.66
604	0	45.640	91.256	91.240	91.256	91.240	13.2	19.9	22.66
606	0	45.640	91.256	91.240	91.256	91.240	7.7	7.7	22.66
610	0	45.638	91.252	91.237	91.253	91.237	6.2	8.2	22.66
611	0	45.638	91.253	91.238	91.254	91.238	15.3	21.2	22.66
614	0	45.638	91.253	91.238	91.254	91.238	27.7	25.4	22.66
620	0	45.639	91.227	91.212	91.228	91.212	1.9	3.4	19.63
621	0	45.642	91.244	91.228	91.244	91.229	11.4	14.3	20.92
622	0	45.640	91.251	91.236	91.252	91.236	7.2	9.6	22.10
624	0	45.640	91.263	91.247	91.263	91.247	12.8	17.1	23.28
627	0	45.639	91.258	91.242	91.258	91.243	0.4	1.0	23.05
628	0	45.640	91.261	91.245	91.261	91.246	10.1	13.5	23.02
630	0	45.641	91.262	91.247	91.263	91.247	13.7	15.0	23.01
636	0	45.638	91.250	91.235	91.251	91.235	7.7	7.5	22.34
637	0	45.638	91.252	91.237	91.253	91.237	1.3	4.0	22.76
638	0	45.638	91.255	91.239	91.255	91.240	10.9	14.7	22.95
639	0	45.638	91.257	91.241	91.257	91.242	12.7	18.8	23.17
641	0	45.638	91.250	91.235	91.251	91.235	10.8	18.1	22.42

continued									
643	0	45.638	91.252	91.236	91.252	91.236	15.5	19.4	22.65
644	0	45.638	91.252	91.237	91.253	91.237	5.8	6.2	22.78
646	0	45.638	91.251	91.235	91.251	91.236	7.9	10.3	22.54
647	0	45.638	91.256	91.240	91.256	91.241	6.7	9.6	22.97
648	0	45.638	91.256	91.241	91.257	91.241	5.7	9.1	23.05
649	0	45.638	91.254	91.238	91.254	91.239	0.6	1.1	22.90
650	0	45.643	91.265	91.249	91.265	91.250	6.0	7.4	22.97
651	0	45.639	91.259	91.243	91.259	91.244	0.1	0.3	23.05
652	0	45.639	91.257	91.241	91.257	91.242	6.3	10.0	23.06
654	0	45.639	91.256	91.241	91.257	91.241	9.0	8.9	22.84
655	0	45.639	91.255	91.239	91.255	91.240	5.8	4.7	22.81
656	0	45.639	91.255	91.239	91.255	91.240	2.5	3.9	22.63
658	0	45.639	91.256	91.240	91.256	91.241	3.5	7.1	22.85
659	0	45.639	91.258	91.243	91.259	91.243	15.3	15.9	23.17
661	0	45.639	91.257	91.242	91.258	91.242	6.4	6.5	23.00
662	0	45.637	91.251	91.236	91.252	91.236	7.4	17.5	22.69
678	0	45.638	91.243	91.228	91.244	91.228	8.5	5.4	21.69
679	0	45.639	91.249	91.234	91.250	91.234	5.2	2.8	22.04
680	0	45.638	91.252	91.236	91.252	91.236	12.4	13.6	22.58
683	0	45.638	91.249	91.233	91.249	91.233	3.6	2.9	22.18
690	0	45.639	91.254	91.238	91.254	91.239	4.5	1.9	22.61
691	0	45.639	91.257	91.241	91.257	91.242	9.0	6.8	23.02
692	0	45.641	91.262	91.246	91.262	91.247	5.4	10.1	23.10
693	0	45.638	91.254	91.238	91.254	91.239	6.9	8.0	22.80
696	0	45.635	91.240	91.225	91.241	91.225	8.9	9.1	22.01
697	0	45.637	91.249	91.234	91.250	91.234	2.8	5.3	22.54
699	0	45.635	91.249	91.233	91.249	91.234	18.4	16.6	22.99
700	0	45.635	91.249	91.234	91.250	91.234	15.4	15.9	23.00
704	0	45.636	91.245	91.230	91.246	91.230	13.3	12.8	22.37
707	0	45.636	91.245	91.230	91.246	91.230	10.7	7.7	22.34
709	0	45.636	91.252	91.236	91.252	91.237	8.8	8.9	23.00
711	0	45.636	91.252	91.236	91.252	91.237	7.9	7.6	23.00
716	0	45.636	91.250	91.234	91.250	91.235	4.9	2.6	22.84
718	0	45.633	91.239	91.224	91.240	91.224	7.3	4.9	22.35
725	0	45.636	91.249	91.234	91.250	91.234	10.0	10.1	22.78
727	0	45.637	91.250	91.235	91.251	91.235	11.9	10.4	22.71
728	-1	45.136	90.255	90.240	90.256	90.240	9.3	8.1	23.17
730	0	45.637	91.251	91.235	91.251	91.236	4.3	4.2	22.73
731	0	45.637	91.256	91.240	91.256	91.241	5.8	3.2	23.34
746	0	45.632	91.219	91.204	91.220	91.204	6.2	4.7	22.54
748	0	45.634	91.226	91.211	91.227	91.211	10.6	14.1	22.91
749	1	46.008	91.972	91.957	91.973	91.957	8.7	6.5	22.89
750	1	46.009	91.968	91.953	91.969	91.953	6.3	10.5	22.39
752	0	45.634	91.225	91.210	91.226	91.210	12.3	14.2	22.78
754	-2	44.759	89.480	89.465	89.481	89.465	10.8	11.8	22.79
756	0	45.636	91.229	91.214	91.230	91.214	11.3	14.1	22.93
758	2	46.510	92.972	92.957	92.973	92.957	10.2	12.2	22.75
759	0	45.635	91.230	91.215	91.231	91.215	9.5	13.1	23.13
760	-3	44.260	88.486	88.471	88.487	88.471	9.5	6.4	23.06
761	0	45.635	91.230	91.214	91.230	91.214	7.2	7.1	23.05
763	3	46.886	93.723	93.708	93.724	93.708	13.3	14.2	22.90
764	0	45.638	91.237	91.221	91.237	91.222	10.1	10.5	23.32
765	-1	45.135	90.235	90.219	90.235	90.220	4.9	6.5	23.30
778	0	45.633	91.220	91.204	91.220	91.205	8.4	10.2	22.34
779	1	46.012	91.981	91.965	91.981	91.966	10.0	12.4	22.90
780	0	45.634	91.229	91.213	91.230	91.214	9.9	11.7	23.19
781	-1	45.134	90.227	90.212	90.228	90.212	1.5	1.4	22.76
782	-1	45.135	90.230	90.215	90.231	90.215	8.7	11.1	22.97

continued									
783	0	45.635	91.230	91.215	91.231	91.215	10.1	14.0	23.17
784	2	46.510	92.977	92.962	92.978	92.962	9.1	13.9	23.34
785	0	45.635	91.228	91.212	91.228	91.213	7.2	11.1	22.96
786	-2	44.760	89.485	89.469	89.485	89.469	9.2	11.3	23.16
788	0	45.634	91.225	91.209	91.225	91.210	3.8	6.1	22.78
789	3	46.884	93.721	93.706	93.722	93.706	8.3	12.6	23.07
790	0	45.635	91.230	91.214	91.230	91.215	9.3	11.8	23.18
791	-3	44.260	88.486	88.470	88.486	88.471	0.8	1.7	22.97
792	-3	44.260	88.486	88.471	88.487	88.471	11.5	13.6	22.99
810	0	45.631	91.205	91.189	91.205	91.190	1.8	3.5	21.25
811	0	45.631	91.206	91.191	91.207	91.191	0.0	0.0	21.45
812	0	45.633	91.213	91.197	91.213	91.198	3.0	3.9	21.65
816	0	45.631	91.198	91.183	91.199	91.183	0.5	0.3	20.54
817	0	45.631	91.203	91.188	91.204	91.188	8.2	10.6	21.16
818	-2	44.756	89.462	89.447	89.463	89.447	1.1	1.2	21.48
819	-2	44.757	89.465	89.450	89.466	89.450	8.2	11.0	21.72
820	0	45.632	91.212	91.197	91.213	91.197	4.3	6.0	21.96
821	2	46.508	92.960	92.944	92.960	92.945	8.9	15.9	21.94
822	0	45.633	91.218	91.203	91.219	91.203	7.8	9.3	22.30
823	-3	44.258	88.478	88.462	88.478	88.463	9.7	13.1	22.50
824	0	45.633	91.220	91.204	91.220	91.204	10.3	18.3	22.39
825	3	46.883	93.709	93.694	93.710	93.694	9.5	16.2	22.13
826	0	45.633	91.218	91.202	91.218	91.203	13.2	19.1	22.16
827	-1	45.133	90.222	90.206	90.223	90.207	13.1	21.3	22.39
828	1	46.008	91.969	91.954	91.970	91.954	11.0	17.2	22.55
830	0	45.634	91.218	91.202	91.218	91.203	12.5	19.5	22.06
831	3	46.883	93.713	93.698	93.714	93.698	11.9	19.9	22.49
832	-3	44.257	88.470	88.454	88.470	88.455	15.6	18.9	21.72
833	0	45.632	91.215	91.199	91.215	91.200	4.4	8.0	22.02
834	2	46.508	92.963	92.947	92.963	92.948	12.1	16.6	22.20
835	-2	44.753	89.462	89.446	89.462	89.447	11.5	18.4	22.15
836	0	45.629	91.211	91.196	91.212	91.196	7.9	13.7	22.45
850	0	45.633	91.213	91.197	91.213	91.198	10.2	9.2	21.75
851	2	46.508	92.965	92.950	92.966	92.950	11.7	15.3	22.38
853	-2	44.759	89.477	89.461	89.477	89.462	9.7	9.9	22.48
854	0	45.632	91.219	91.203	91.219	91.204	9.5	11.9	22.46
855	1	46.008	91.961	91.946	91.962	91.946	9.2	10.3	21.78
856	-1	45.132	90.219	90.204	90.220	90.204	11.0	13.0	22.25
857	0	45.633	91.220	91.204	91.220	91.205	3.0	6.4	22.40
858	0	45.633	91.220	91.204	91.220	91.205	8.2	13.7	22.51
859	3	46.883	93.716	93.700	93.716	93.701	16.0	14.9	22.84
860	-3	44.258	88.481	88.466	88.482	88.466	10.7	15.4	22.91
861	0	45.633	91.223	91.207	91.223	91.207	9.0	10.8	22.74
862	1	46.003	91.960	91.945	91.961	91.945	11.0	18.6	22.71
863	-1	45.127	90.213	90.198	90.214	90.198	0.2	0.3	22.70
864	-1	45.130	90.217	90.202	90.218	90.202	10.7	16.6	22.52
866	-2	44.755	89.463	89.449	89.464	89.449	10.4	15.6	22.02

D Temperature distributions

Temperature distribution weighted with luminosity (in $mA^2 \times$hours) in 0.1 ^{0}C bins for each of the seven energy points of the 1991 scan, fills 678 to 866.

Mean	energy point in the scan						
Temp.	-3	-2	-1	0	1	2	3
20.5	0.00000	0.00000	0.00000	0.26640	0.00000	0.00000	0.00000
20.6	0.00000	0.00000	0.00000	0.00000	0.00000	0.00000	0.00000
20.7	0.00000	0.00000	0.00000	0.94855	0.00000	0.00000	0.00000
20.8	0.00000	0.00000	0.00000	0.89726	0.00000	0.00000	0.00000
20.9	0.00000	0.00000	0.00000	1.44731	0.00000	0.00000	0.00000
21.0	0.00000	0.00000	0.00000	1.71978	0.00000	0.00000	0.00000
21.1	0.00000	0.00000	0.00000	2.46059	0.00000	0.00000	0.00000
21.2	0.00000	0.00000	0.00000	2.82777	0.29178	0.00000	0.00000
21.3	0.00000	0.00000	0.00000	3.09652	0.84410	0.00000	0.00000
21.4	5.79709	1.15838	0.00000	1.66795	1.50180	0.00000	0.00000
21.5	0.72329	2.86879	0.00000	3.75964	0.71761	0.00000	0.00000
21.6	2.69182	0.87888	0.00000	1.67921	0.72458	1.42679	0.00000
21.7	3.16680	8.15738	0.00000	1.86377	1.26859	2.94480	0.00000
21.8	1.10182	2.85285	0.00000	6.66645	1.15463	2.12936	0.00000
21.9	0.98935	2.79762	0.00000	14.72415	0.90919	3.34166	5.63002
22.0	1.78675	11.44719	2.79064	12.75150	2.29200	5.93532	2.06640
22.1	1.94039	3.23414	1.56877	12.50159	1.81885	8.71005	1.81028
22.2	1.01493	7.69537	13.11966	30.86016	2.17079	11.96258	5.41023
22.3	2.00170	3.96724	5.05872	12.94199	1.96638	2.39190	3.69452
22.4	3.34298	5.70051	12.67195	28.74097	5.68618	5.83199	6.77770
22.5	1.55931	4.98657	9.55106	25.37988	13.51330	3.69820	7.99668
22.6	5.86537	2.72700	2.93670	19.13971	7.80537	3.08209	7.33960
22.7	2.47518	3.77942	8.33238	28.61497	18.17205	3.12965	8.51139
22.8	1.96776	0.53554	1.09211	12.85093	3.44940	0.80950	2.37412
22.9	20.21682	1.93758	1.91714	12.18192	4.28954	1.79434	8.06873
23.0	4.78919	3.10701	3.67988	24.00605	4.33220	2.21911	4.64694
23.1	4.92783	6.22184	4.44983	25.85469	2.71097	0.47443	6.29060
23.2	2.74479	5.09832	9.83387	40.43897	0.00000	6.67812	7.11288
23.3	0.00000	0.00000	0.58508	1.61712	0.00000	1.63348	0.00000
23.4	0.00000	0.00000	0.57145	2.49470	0.00000	5.57989	0.00000
23.5	0.00000	0.00000	0.00000	0.29107	0.00000	0.00000	0.00000